On the Solution Structure of PHB: Preparation and NMR Analysis of Isotopically Labeled Oligo[(*R*)-3-hydroxybutanoic Acids] (OHBs)

by **Peter Waser**[1]), **Magnus Rueping**[2]), and **Dieter Seebach***)

Laboratorium für Organische Chemie der Eidgenössischen Technischen Hochschule, ETH-Zentrum, Universitätstrasse 16, CH-8092 Zürich

and

Elke Duchardt[3]) and **Harald Schwalbe***[4])

Department of Chemistry, Francis Bitter Magnet Laboratory, Massachusetts, Institute of Technology, 170 Albany Street, Cambridge, MA 02139, USA

Dedicated to Professor *Edgar Heilbronner* with best wishes on the occasion of his 80th birthday

While the chain conformation of poly- and oligo[(*R*)-3-hydroxybutanoate] (PHB, OHB) is known to be 2_1- and 3_1-helical in stretched fibers and in the crystalline state, respectively (*Fig. 2*), the structure in solution is unknown. To be able to determine the NMR-solution structure, specifically labeled linear oligomers have been prepared: a 16-mer consisting of alternating pairs of fully ^{13}C-labeled and non-labeled residues (**1**) and a 20-mer containing an *O*-^{13}CH(^{13}CH$_2$D)-^{13}CHD^{Si}-^{13}CO residue in position 9 (from the *O*-terminus) and a fully ^{13}C-labeled residue in position 12 (**2**), both with (*t*-Bu)Ph$_2$Si protection at the O- and Bn protection at the C-terminus. The labeled (*R*)-3-hydroxybutanoic acid building blocks were prepared by *Noyori* hydrogenation of the ethyl ester of fully ^{13}C-labeled acetoacetic acid, and the D-atoms were incorporated by D$_2$/Pd-C reduction of a previously reported dibromo-1,3-dioxinone **8** (*Scheme 1*). The oligomers were obtained by a series of fragment couplings (*Schemes 2* and *3*). 600-MHz NMR COSY, HSQC, ROESY, and cross-correlated relaxation measurements (*Figs. 4–6*, *9*, and *12*, and *Tables 1–3*) at different temperatures and interpretations thereof led to assignments of all resonances, including those from the diastereotopic C(2)H$_2$ protons, and to determination of the conformationally averaged dihedral angles ϕ_2 and ϕ_3 (*Figs. 2*, *7*, and *8*) in the chain of the oligoester. The conclusions are: all but five or six terminal residues adopt the same conformation; the 2_1 helix is *not* the predominant secondary structure; the structure of the HB chain is averaged, even at –30°. Our investigation confirms the high flexibility of the polyester chain, a property that has been deduced previously from biological studies of PHB in membranes, in ion channels, and as appendage of proteins.

Introduction. – The biopolymer poly[(*R*)-3-hydroxybutanoic acid] (PHB) is a microbial storage material of high molecular weight (*ca.* 10^6 Da [1]). Short-chain derivatives (*ca.* 12×10^3 Da, corresponding to 150 residues) have been shown to form, or be part of, ion channels through planar or liposomal phospholipid bilayers and cell walls [2]. The actual structure of the PHB that causes the ion-transporting effect is unknown. Several models have been proposed for the ion channels or pores involving PHB [3] (*Fig. 1*). These are derived from modeling [4] or from the known PHB structures in stretched fibers [5], in lamellar crystallites [6], and in single crystals of

1) Part of Dissertation Nr. 13552 of *P. W.*, ETH-Zürich, 2000.
2) Part of the projected Ph. D. thesis of *M. R.*, ETH-Zürich.
3) Part of the projected Ph. D. thesis of *E. D.*, MIT, Cambridge, USA.
4) Correspondence author for the NMR part. We acknowledge stimulating discussions with Prof. *C. Griesinger*.

cyclic oligomers [7] (*Fig. 2*). Since the phospholipid bilayer may be considered a two-dimensional nonpolar solvent covered on both sides by a layer of charged, polar groups, the structure of PHB in solution must be elucidated. We have recently reported the CD spectra of oligo(hydroxybutanoic acids) (OHBs), containing 8, 16, and 32 HB units in homogeneous solution, and in a bilayer consisting of racemic phospholipids [8]. The observed *Cotton* effects near 210 nm are an indication for the presence of chiral secondary structures in the ensemble of molecules – on the very short time scale of UV spectroscopy. Also, FRET measurements with doubly fluorescence-labeled OHBs of various chain lengths in 10^{-6} M solutions provide distances between the *termini*, which are compatible with folded conformations of the intermediate chains [8], again on the short time scale of UV/VIS spectroscopy[5]).

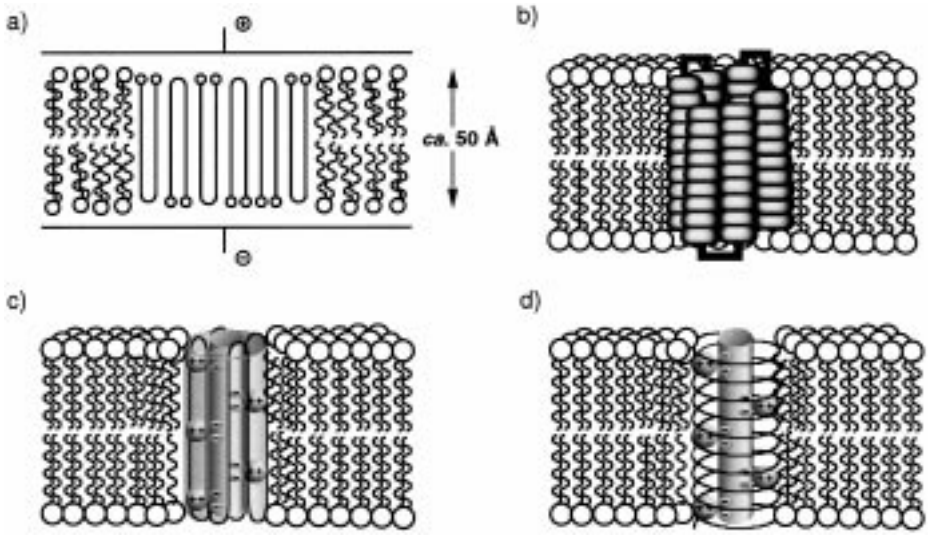

Fig. 1. *Proposed structures of ion channels consisting of or containing short HB chains.* Hairpins of HB 32mers (in a 2_1-helical conformation of the chain) have been proposed to form aggregates for ion transport through phospholipid bilayers by a single-channel (*a*) or by a pore mechanism (*b*) [3][8]. Calcium polyphosphate (chain lengths *ca.* 75 units) complexes with PHB (*ca.* 150 units) form Ca-specific channels for which structures *c* and *d* have been proposed [4][3].

It would be desirable to determine the NMR-solution structure of PHB chains – if the highly flexible polyester chain has a preferred conformation at all on the rather long time scale of this spectroscopy. Qualitatively, the NMR spectra of cyclic and linear OHBs [10] look very similar, exhibiting only one set of average signals for all the residues. Thus, the cyclic hexamer, a 24-membered ring, that exists in crystals in a folded and twisted conformation resembling the number 8 (*Fig. 3*) has an ^{1}H-NMR spectrum with only one set of sharp signals from the $CH(CH_3)CH_2$ protons (*Fig. 3*). This means that the molecule has C_6 geometry on the NMR time scale.

To obtain more detailed information about the conformation of linear HB oligomers by NMR spectroscopy in solution, we have now prepared the alternatingly

[5]) For review articles covering the chemistry, structure and biology of PHB, see [9].

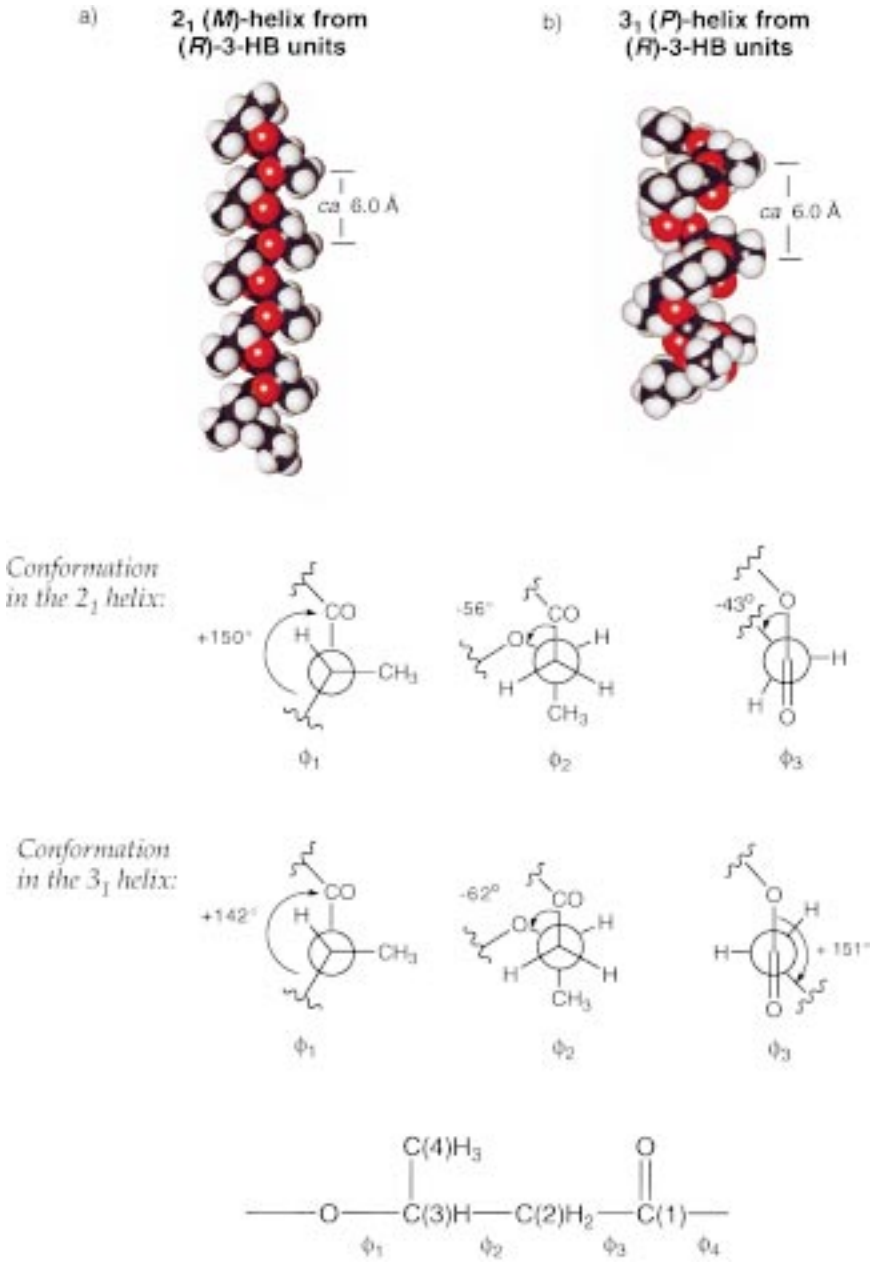

Fig. 2. *Models for the structure of PHB and OHB chains.* The 2_1 helix (*a*) has been determined by fiber X-ray diffraction of PHB [5], the 3_1 helix (*b*) is constructed from single helix turns seen in crystal structures of cyclic oligomers of HB. Torsion angles ($\phi_1 - \phi_4$) and corresponding *Newman* projections of both preferred HB-conformations from crystal structures of macrolides [7].

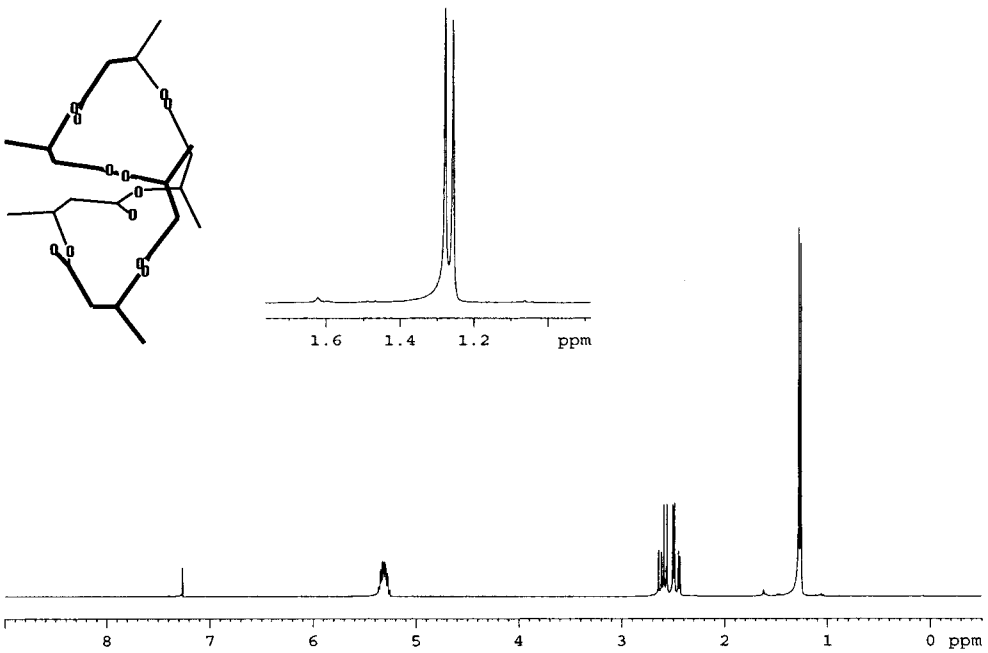

Fig. 3. *^{1}H-NMR Spectrum of the cyclic HB-hexamer (hexolide)*. One set of $CH(CH_3)CH_2$ resonances indicates that the compound has a C_6 symmetry on the NMR time scale, while it is twisted and folded (as shown) in the solid state.

^{13}C-labeled 16-mer **1** and the specifically ^{2}H- and ^{13}C-labeled 20-mer **2**, hoping that the magnetic labels would enable us to determine the local angles of the HB residues (from coupling constants and cross-correlated relaxation rates) and the overall conformation of the chain (*via* ROE intensities). The positions with an asterix in the formulae **1** and **2** are ^{13}C-atoms.

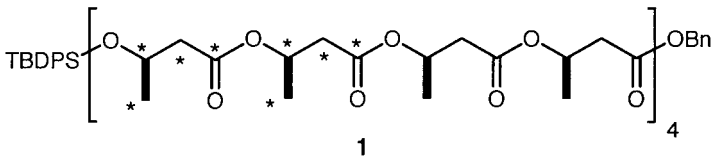

1

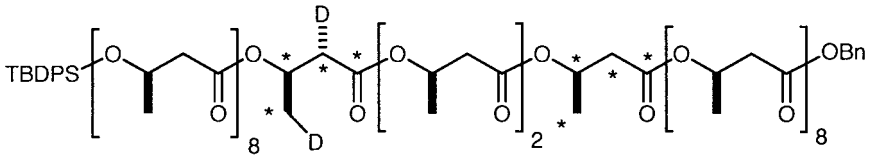

2

2. Synthesis of the Isotopically Labeled OHBs. – We have previously reported the synthesis of linear oligomers of HB up to a chain-length of 128 residues by fragment coupling [11]. The syntheses started from (*R*)-3-hydroxybutanoic acid, as obtained from the commercial PHB. The fragments were protected orthogonally by (*t*-Bu)Ph_2Si on the O-terminus and by CH_2Ph on the C-terminus, so that selectively mono-protected intermediates (*t*-Bu)$Ph_2Si-(OCHMeCH_2CO)_n-OH$ and $H-(OCHMe-CH_2-CO)_n-OBn$ are readily available for coupling ($(COCl_2)$ activation/pyridine in CH_2Cl_2, with warming from $-78°$). Thus, the specifically labeled fragments had to be prepared and coupled to give the desired OHBs **1** and **2**. To this end (*Scheme 1*), commercial ethyl 3-oxo-butanoate **3***, which was labeled $\geq 99\%$ on each of the four butanoate C-atoms (by ^{1}H-NMR analysis) was hydrogenated under *Noyori* conditions [12] ((*M*)-BINAP/$RuBr_2$ catalyst/H_2 [13]) to give the labeled (*R*)-3-hydroxybutanoate **4*** of 99.3% enantiomer purity in 96% yield. Protection of the OH group and conversion of the ethyl to the benzyl ester **5*** was achieved in an overall yield of 77% (from the commercial acetoacetate **3***, on a 6-g scale). Debenzylation (H_2/Pd-C) of half of the material ($\rightarrow$ **6***) and desilylation (HF · pyridine) of the other half ($\rightarrow$ **7***), with subsequent coupling gave the labeled *O*-silyl- and *C*-benzyl-protected 'dimer'

Scheme 1. *Preparation of the* (R)*-3-Hydroxybutanoic Acid Derivatives* **6***, **7***, *and* **9** *for the Assembly of Labeled OHBs*

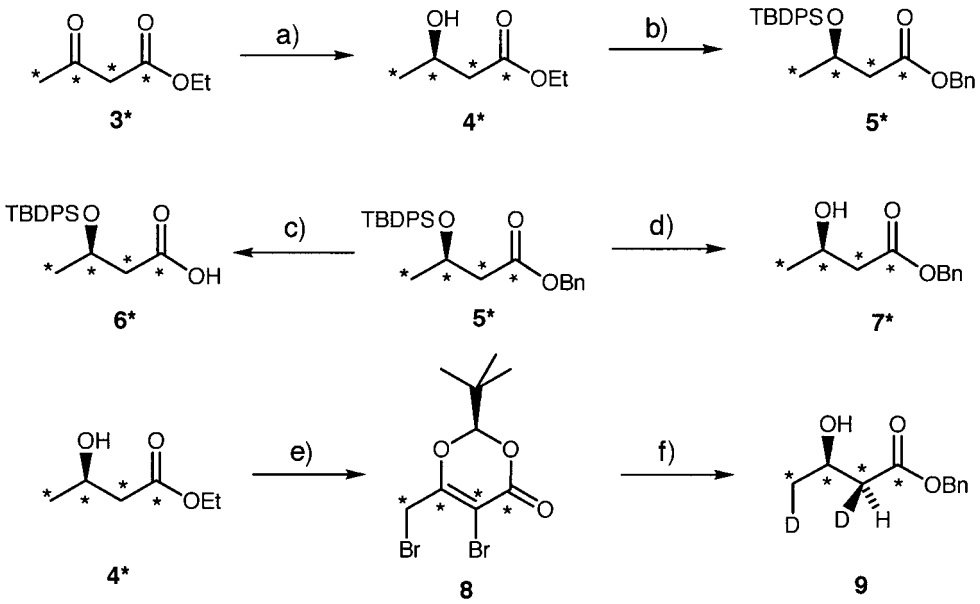

a) [Ru((*M*)-BINAP)Br_2], 85 atm H_2, EtOH, b) TBDPSCI, DMAP, DMF; KOH, EtOH; BnBr, Na_2CO_3, DMF. c) H_2, Pd/C in MeOH. d) HF-pyridine, CH_2Cl_2. e) 1N KOH; Me_3SiOTf, Et_3N, Me_3CCHO; NBS, AIBN, CCl_4. f) D_2, C_6H_6, Pd/C; H_2, Pd/C; *Dowex,* MeOH/H_2O; BnBr, Na_2CO_3, DMF. Abbreviations: AIBN = 2,2′-azo[isobutyronitril]. BINAP = 2,2′-Bis(diphenylphosphino)-1,1′-binaphthalene, TBDPS = (*t*-Bu)Ph_2Si, DMAP = 4-(Dimethylamino)pyridine, Bn = $PhCH_2$, TBDMS = (*t*-Bu)Me_2Si, Tf = trifluoromethylsulfonyl, NBS = *N*-bromosuccinimide.

Scheme 2. *Preparation of the* ^{13}*C-Labeled Oligomers* **13** *and* **14** (containing four and eight HB units, respectively), *Intermediates on the Way to the Hexadecamer* **1** *with Specific Labeling on Eight Positions*

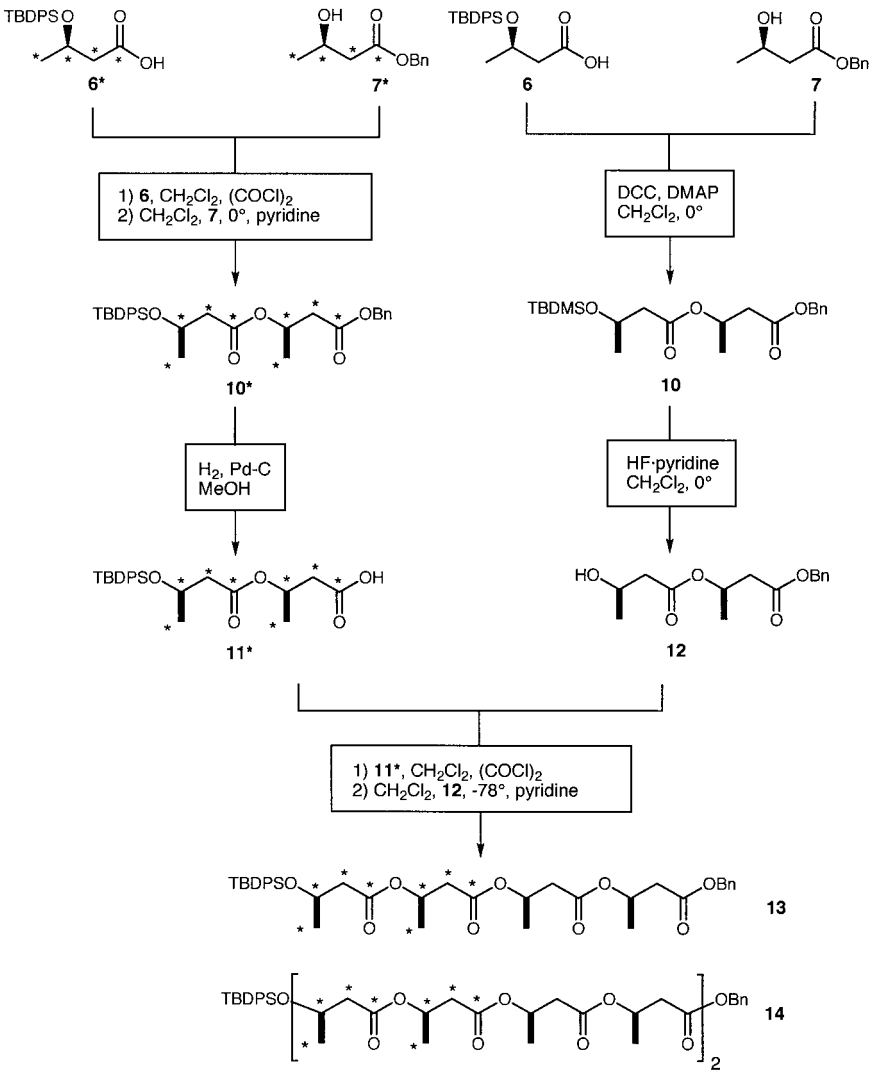

10* (80%), ready to be channeled into fragment-coupling processes (*Schemes 2* and *3*).

The ^{2}H- and ^{13}C-labeled hydroxy-butanoate **9** was prepared through the dibromo-dioxinone **8**. This compound – unlabeled – had been used by us previously as an intermediate on the way to the 2-(*tert*-butyl)-6-methyl-1,3-dioxin-4-one [14]; Br/D-exchange (D_2/Pd-C in C_6H_6) and hydrogenation from the face *trans* to the *t*-Bu group [15] gave the desired specifically labeled compound **9** in an overall yield of *ca.* 12% from ester **4***, in eight steps, the poorest one being the bromination with NBS [16],

Scheme 3. *Principle of Fragment Coupling for OHB Synthesis and Intermediates* **15**–**18** *on the Way to the Icosamer* **2**. Fully (silyl and benzyl) protected oligomers are converted to the *O*-Si-protected oligo-acids **A** or hydroxy oligo-esters **B**. These are coupled to give the larger, fully protected oligomers **C**.

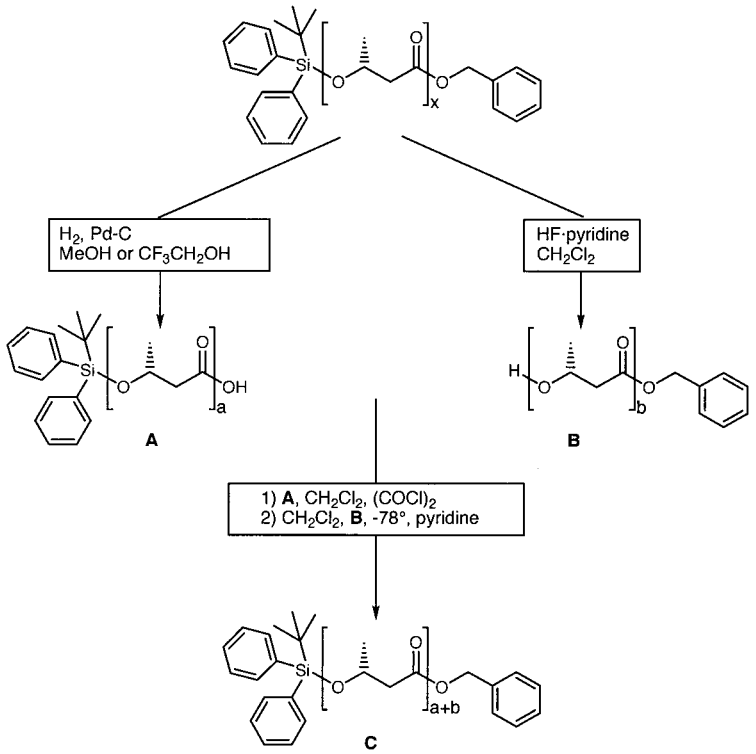

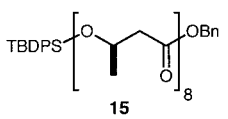

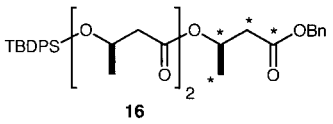

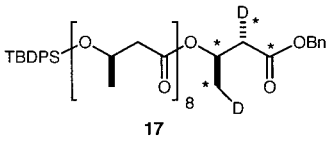

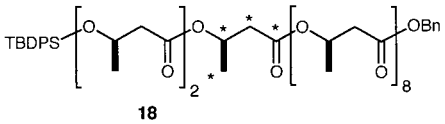

which gave only 24% of purified **8**. Perhaps not surprisingly, there was some over-deuteration in the Br/D exchange step, placing more than one D into the Me group at C(4) of the ester **9** (degree of deuteration 0.42 instead of 0.33). On the other hand, the hydrogenation of the C=C bond was surprisingly clean and diastereoselective: the

ester **9** was of 91% enantiomer purity and contained 99% of D at C(2) in the *Si*-position[6]).

The subsequent assembly of the target molecules **1** and **2** was achieved by applying the previously published fragment coupling [11], which is schematically outlined in *Scheme 3*. Thus, the nonlabeled *O*-TBDPS-protected hydroxy acid **6** and benzyl ester **7** were coupled to the 'dimer' **10**, *O*- and *C*-terminal deprotection of **10** and **10*** (→ **12**, **11***), respectively, and, again, coupling gave the 'tetramer' **13** with two labeled and two nonlabeled HB units (*Scheme 2*). Two rounds of fragment coupling (*Scheme 3*) with the $(HB)_4$ derivatives **13** (→ **14** → **1**) gave the protected target hexadeca[(*R*)-3-hydroxybutanoate] **1** with alternating pairs of ^{13}C-labeled and unlabeled units.

For the assembly of the specifically ^{2}H- and ^{13}C-labeled icosa(hydroxybutanoate) **2**, we used the building blocks **15**, containing eight HB units [11], and the protected 'dimer' **10** [11]. Following the fragment-coupling scheme, **10** was debenzylated (→ **11**) and combined with the labeled hydroxy ester **7*** to give the 'trimer' **16**, which, in turn, was debenzylated and connected with the *O*-desilylated 8-mer derivative **15** to give **18**, containing 11 HB units. On the other end, the debenzylated 8-mer derivative **15** was elongated with the ^{2}H- and ^{13}C-labeled benzyl 3-hydroxybutanoate **9** to give the 'nonamer' **17**. Ester formation between the C-terminal hydroxy acid residue of debenzylated **17** and the O-terminal residue of desilylated **18**, finally, provided the desired 20-mer derivative **2** (*Scheme 3*).

3. NMR Analysis: Spectral Assignment. – The ^{1}H-1D and the COSY spectra of the 16-mer **1** are shown in *Fig. 4* together with the spectral assignment. The resonances of all repetition units overlap except for three ^{12}C- and three ^{13}C-labeled units. Because of ROE signals to aromatic protons, the unit comprising the $C(2)H_2$ protons at *ca.* 4 ppm is assigned to be the O-terminal residue 1. This unit shows $C(4)H_3$,$C(2)H_2$ cross-peaks to the non-bulk ^{13}C-labeled unit that is resonating close to bulk-frequency, which is, therefore, assigned to be the subsequent O-terminal residue 2. The third resolved ^{13}C-labeled unit that also gives rise to $C(2)H_2$ resonances at *ca.* 4 ppm is of minor intensity and does not show any interresidual cross peaks.

Assignment of the non-bulk ^{12}C units, which resonate close to the bulk resonances, cannot be performed due to missing interresidual cross-peaks. However, it is likely that they are the two C-terminal units and the first ^{12}C unit adjacent to the O-terminus.

The extent of signal overlap in the 20-mer is about the same as in the 16-mer. However, the ^{13}C-HSQC (*Fig. 5*) shows that the two ^{13}C-labeled units can be discriminated because of the primary isotope shift of C(4) and C(2), as well as the secondary isotope shift of the remaining $C(2)H_2$ and $C(4)H_3$ protons in the deuterated unit (CHD) relative to the respective resonances in the nondeuterated unit (CH_2). In addition, the difference in *multiplet* structure of the $C(4)H_3$ and the $C(2)H_2$ cross-peaks of the two units in the indirect detected dimension in the ^{13}C- and ^{2}H-coupled spectrum further resolves the spectrum. For instance, the $C(3)H$,$C(2)H_2$ cross-peaks are split by two times $^{1}J_{(C,H)}$ in the indirect detected dimension, due to the $^{1}J_{(C,H)}$ coupling to two protons during this time period. The C(2)HD,C(3)H cross-peak, in contrast, is split by

---

[6]) For a detailed analysis by ^{1}H- and ^{13}C-NMR spectroscopy and high-resolution mass spectrometry, we refer the reader to the dissertation of *P. W.*[1]). See also the NMR part of this paper.

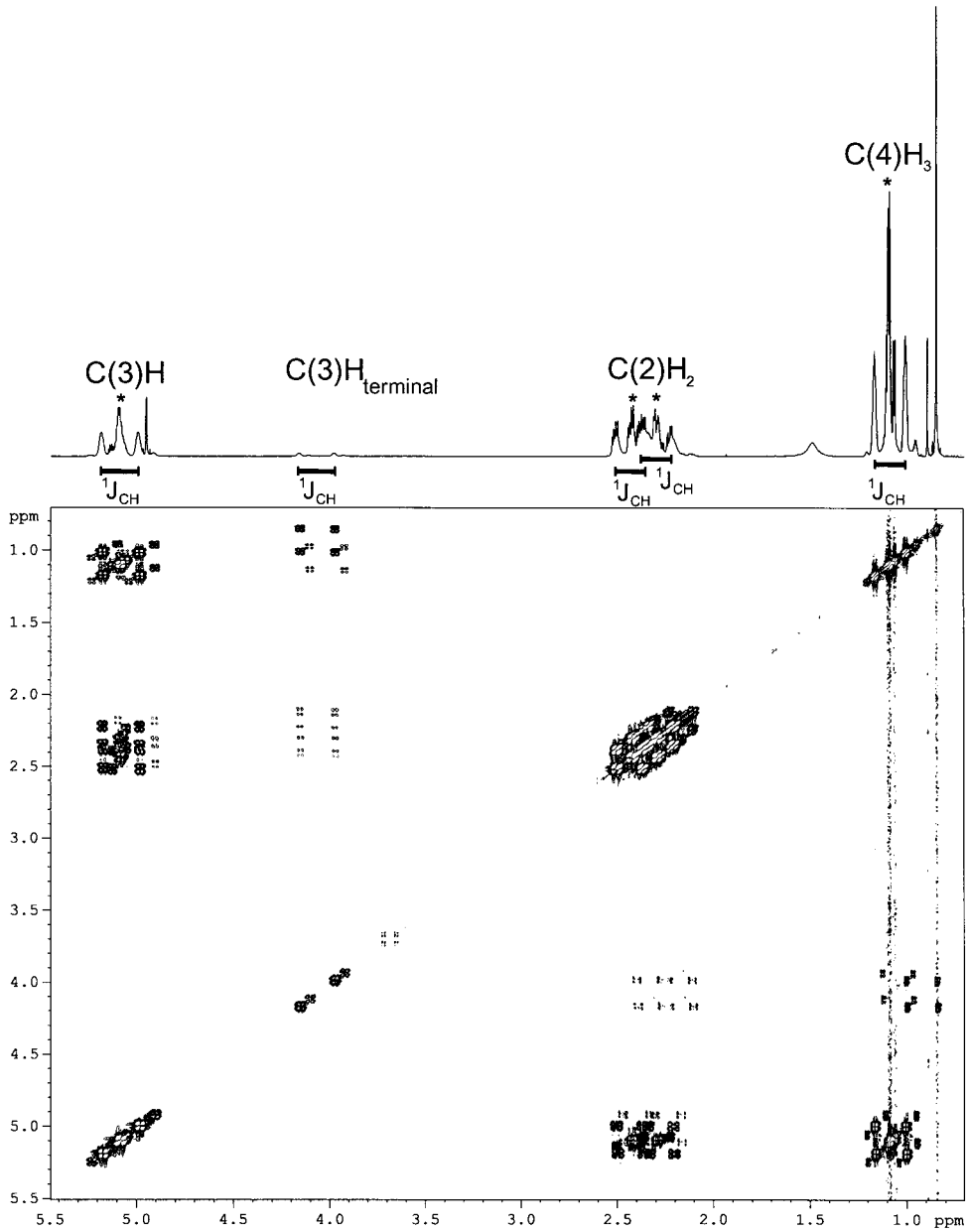

Fig. 4. *^{1}H-1D and ^{1}H-DQF-COSY spectra of the 16-mer* **1** *without carbon decoupling in* t_1 *and* t_2. The spectral assignment is given in the 1D; ^{12}C-bound protons are indicated with an asterisk*, for the resonances originating from ^{13}C-bound protons, the splitting due to the $^1J_{(C,H)}$ coupling is indicated.

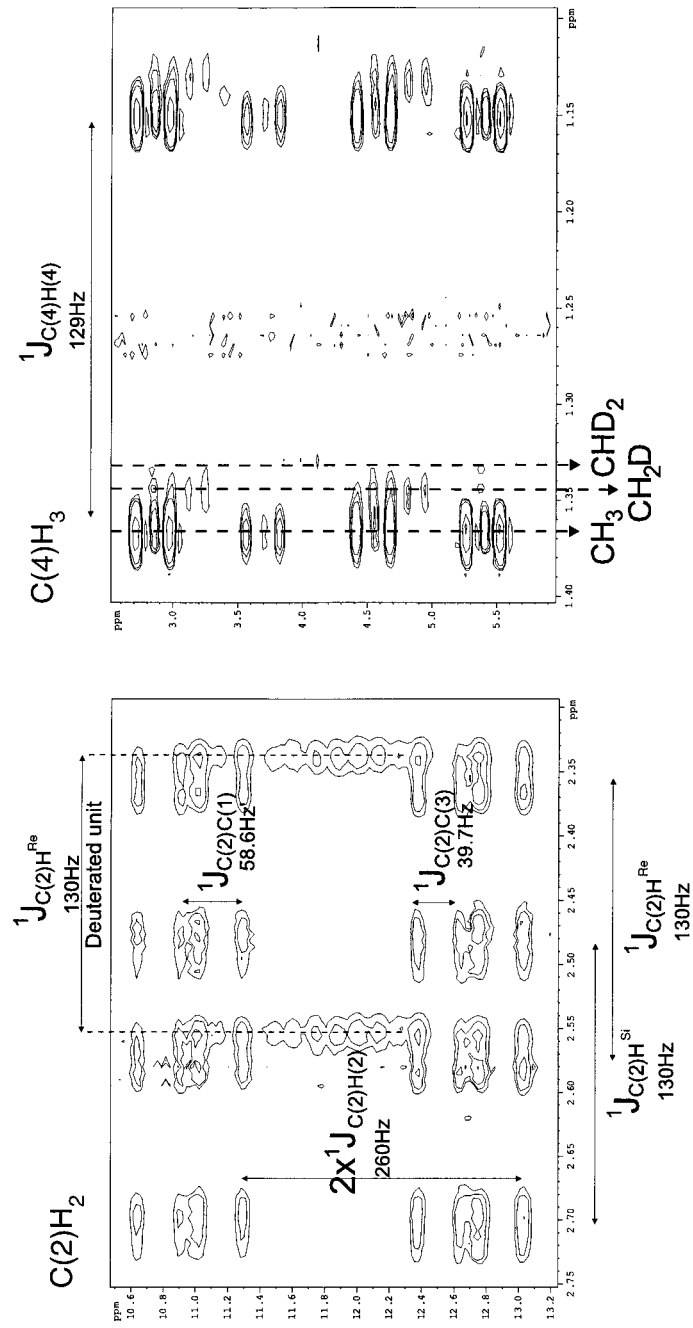

Fig. 5. *^{13}C-HSQC Spectrum of the 20-mer* **2**. The C(2)H_2 (*left*) and the C(4)H_3 regions (*right*) are enlarged. The spectrum is not decoupled (^{1}H,^{2}H in t, ^{13}C, ^{2}H in t_2), and interesting couplings are indicated. In the ^{1}H-dimension, all resonances are split by the respective $^1J_{(C,H)}$ coupling and by several additional long-range couplings. In the ^{13}C-dimension, the C(2)H cross-peak of the CHD unit is split by $^1J_{(C,H)}$ and additional ^{2}H,C and C,C couplings. Due to the presence of the spin 1 nucleus ^{2}H, C(2) experiences quadrupolar relaxation, which results in a differential weakening of the *multiplet* components of the resonance. The C(2)H resonances of the CH_2 unit are split by two times $^1J_{(C,H)}$ (for an explanation, see text) as well as by the $^1J_{(C(2),C(3))}$ and the $^1J_{(C(1),C(2))}$ coupling in ω_1. For the C(4)H_mD_n resonances, three different isotopomers can be discriminated due to D secondary isotope shifts of their ^{1}H chemical shifts as well as their characteristic *multiplet* splitting. The resonance from the CH_3 group of the nondeuterated unit and the CH_3 isotopomer in the deuterated unit overlap, while the CH_2D and the CHD_2 isotopomers of the deuterated unit are resolved as indicated. The spectrum has been recorded on a *Bruker* 600-MHz spectrometer with a spectral width of 2000 Hz and 256 complex points in the ^{13}C-dimension and 6000 Hz and 1024 complex points in the ^{1}H dimension.

only $^1J_{(C,H)}$, since the C couples to one H only. Further splittings and additional relaxation effects arise due to the presence of the D. A distinct coupling pattern is observed for the three different $C(4)H_nD_m$ isotopomers shown with the relevant 1D slices from the ^{13}C-HSQC spectrum in *Fig. 6*.

Assignment of the Diastereotopic $CH_2(2)$ Protons. To determine ϕ_2, the two diastereotopic $C(2)H_2$ protons have to be stereospecifically assigned. In the case of the 20-mer, one of the ^{13}C-labeled units is stereospecifically deuterated at the $C(2)H^{Si}$-position. Since the remaining C(2)H proton resonates at an upfield chemical shift, this proton is $C(2)H^{Re}$, and the downfield proton is $C(2)H^{Si}$. To stereospecifically assign the $C(2)H_2$ protons (independently of this 'synthetic information'), vicinal coupling constants have been measured and interpreted for the 16-mer **1** and for the 20-mer **2**. The three possible conformations (*ap*, (−)- and (+)-*sc*) around the ϕ_2 are shown in *Fig. 7* together with the characteristic relative sizes of homo- and heteronuclear coupling constants.

Since both $^3J_{(C(4),C(2)H)}$-coupling constants are close to zero and $^3J_{(C(1),C(3)H)}$ is also small, while $^3J_{(C(2)H,C(3)^{Down})}$ is larger than $^3J_{(C(2)H,C(3)H^{Up})}$ in the bulk units for both compounds (*Table 1*), the predominant conformation around the ϕ_2 angle is (−)-*sc*. In agreement with the diastereospecific synthesis, this leads to the following assignment: $C(2)H^{Down}$ is $C(2)H^{Si}$, and $C(2)H^{Up}$ is $C(2)H^{Re}$. This stereospecific assignment is opposite to that reported by *Doi* and co-workers for dimers and trimers of HB (no stereospecific assignment has been performed in this investigation) [17].

Table 1. *Homo- and Heteronuclear Coupling Constants in the Resolved Units of the 16-Mer* **1** *and the 20-Mer* **2**. n.d. = not determined. The data were determined from HCCH-E.COSY experiments [20].

Parameter	16-Mer			20-Mer	
	Bulk	Terminal residue 1	Terminal residue 2	CH_2	CHD
$^3J(C(3)H,C(2)H^{Down,Si})$	7.3 Hz	6.4 Hz	7.2 Hz	7.4 Hz	n.d.
$^3J(C(3)H,C(2)H^{Up,Re})$	5.7 Hz	6.9 Hz	6.7 Hz	5.5 Hz	5.6 Hz
$^3J(C(2)H^{Down,Si},C(4))$	2.6 Hz	n.d.	n.d.	0.1 Hz	n.d.
$^3J(C(2)H^{Up,Re},C(4))$	0.6 Hz	1.5 Hz	n.d.	0.4 Hz	0.4 Hz
$^3J(C(3)H,C(1))$	2.7 Hz	2.8 Hz	2.6 Hz	3.2 Hz	n.d.

For the two ^{13}C-labeled O-terminal units of the 16-mer, the assignment of the chemical shifts of the diastereotopic $C(2)H_2$ protons is identical, although the relative size of the $^3J_{(C(2)H,C(3)H)}$-coupling constants is reversed.

Conformational Analysis: Backbone Angle ϕ_2. In both helices, the torsion angle ϕ_2 is close to the (−)-*sc* conformation (-62.4° for a 2_1 and -52.1° for a 3_1 helix). The $^3J_{(C(2)H,C(3)H)}$-coupling constants (*Table 1*) show that the conformation around ϕ_2 is averaged for both compounds **1** and **2**. The populations of the different rotamers are given in *Table 2*. A detailed description of the coupling-constant analysis is given in the caption of *Table 2*.

In all of the bulk-residues, the (−)-*sc*-conformation is populated by *ca.* 55%. The highest possible helix content is, therefore, *ca.* 0.55^n, with n being the number of residues involved in the helix (*e.g.*, for 5 3-HB-units, the possible helix content is *ca.*

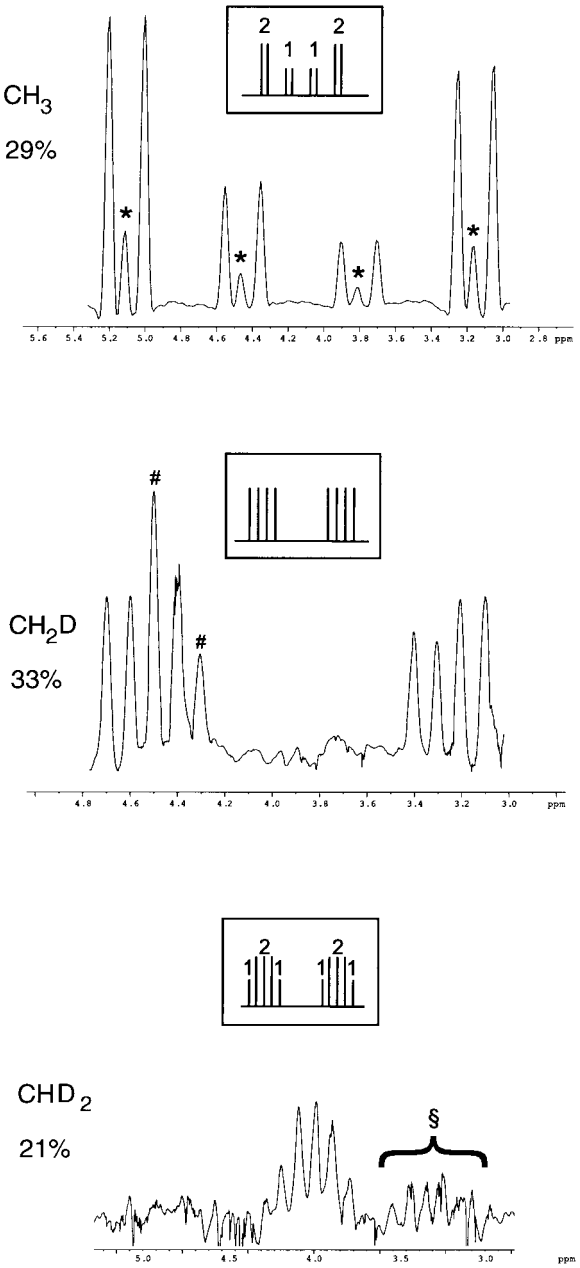

Fig. 6. *1D Slices of the* ^{13}*C-HSQC spectrum depicted in* Fig. 5 *at the frequency of the different* $C(4)H_mD_n$ *isotopomers* (isotopomeric ratio determined in monomers). The *multiplet* patterns are indicated. Populations of the different species are given. *: ^{13}C-Natural abundance signal from nonlabeled units; #: Partial overlap of signals from different isotopomers; §: Second component of the multiplet weakened due to differential relaxation.

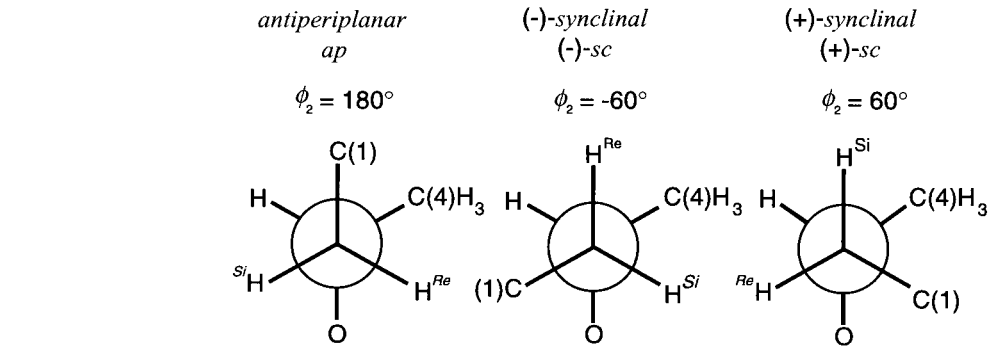

^3J(C(3)H,C(2)H^{Si})	+	**+**	+
^3J(C(3)H,C(2)H^{Re})	**+**	+	+
^3J(C(2)H^{Si},C(4))	**+**	+	+
^3J(C(2)H^{Re},C(4))	+	+	**+**
^3J(C(3)H,C(1))	+	+	**+**

Fig. 7. *The three staggered conformations around* ϕ_2. Relative sizes of the $^3J_{(C(2)H,C(3)H)}$ and $^3J_{(C,H)}$-coupling constants are indicated for each conformation. Bold, large '+' = large relative coupling constant, small '+' = small relative coupling constant.

5%). The conformation of the two O-terminal units (residues 1 and 2) is also averaged, with residue 1 being predominantly in the *ap*-conformation. Residue 2 has a larger population of the (−)-*sc*-conformation (54.9%).

Conformational Analysis: Backbone Angle ϕ_3. The angle ϕ_3 between C(2) and C(1) is the only backbone angle, in which the two proposed secondary structures differ significantly (*Fig. 2*). Due to the lack of neighboring 'NMR-active' nuclei, this angle cannot be analyzed *via* vicinal coupling constants. However, it can be determined from the interpretation of dipole,dipole-CSA cross-correlated relaxation rates between the C(2),C(2)H dipole(s) and the chemical-shift anisotropy (CSA) of the ester C=O group $\Gamma^{DD,CSA}_{C(2),C(2)H,C(1)}$, the value of which depends on the projection angles of the CH-dipole vector(s) onto the different components of the fully anisotropic C(1) chemical-shift tensor as follows [18]:

$$\Gamma^{DD,CSA}_{C(2)C(2)H,C(1)} = 4/15 \frac{h}{2\pi} \frac{\omega_c \gamma_c \gamma_H}{r^3_{CH}} \tau_c f(\sigma_x,\sigma_y,\sigma_z) = \frac{1}{T} \ln \frac{I^D_{DQ} I^U_{ZQ}}{I^D_{ZQ} I^U_{DQ}} \quad (1)$$

ω_C = Carbon *Lamor* frequency
γ_C = Carbon magnetogyric ratio
γ_H = Proton magnetogyric ratio
r_{HC} = C(2)–C(2)H Bond length
τ_C = Rotational correlation time of the molecule
$f(\sigma_x,\sigma_y,\sigma_z) = 0.5\ [\sigma_x(3\cos^2\theta_x - 1) + \sigma_y(3\cos^2\theta_y - 1) + \sigma_z(3\cos\ ^2\theta_z - 1)]$
θ = Angle between the dipole vector and the respective axis of the CSA-tensor.
σ_x, σ_y, σ_z = Principal values of CSA Tensor
$I^{U,D}_{ZQ,DQ}$ = Intensity of upfield (U)/downfield (D) *multiplet* component in the ZQ/DQ spectrum
T = Relaxation delay

The CH-dipole vector(s) are oriented along the CH bond(s). The size of the principle values and the orientation of the ester C=O chemical-shift tensor is known from model compounds [19]. The dependence of $\Gamma^{DD,CSA}_{C(2)C(2)H,C(1)}$ on ϕ_3 is given in *Fig. 8* for the two ^{13}C-labeled residues. The angle dependence of $\Gamma^{DD,CSA}_{C(2)C(2)H,C(1)}$ for the deuterated unit is shifted by 60° relative to the one of the nondeuterated unit, since, in the first case, the relaxation rate depends on the projection angle between the bond vector of the remaining C(2)H proton and the CSA tensor components, while, in the second case, the two C(2),C(2)H vectors are averaged at the position of the vector product. While the rates have the same sign and are of comparable size for both the nondeuterated and the deuterated units, in a 3_1 helix, they have opposite signs and are of different size in a 2_1 helix (*Fig. 8*).

Table 2. $^3J_{(C(3)H,C(2)H)}$-*Coupling Constants and Resulting Populations of the Three Staggered Conformations around* ϕ_2. The populations have been calculated with the *Pachler*-analysis equations: $^3J_{(C(3)H,C(2)H^{Re})} = P_{OG}J_{OG} + P_TJ_T + P_GJ_G$, $^3J_{(C(3)H,C(2)H^{Si})} = P_TJ_{OG} + P_GJ_T + P_{OG}J_G$ and $1 = P_T + P_G + P_{OG}$. J_T, J_O and J_{OG} can be obtained from the generalized *Karplus* equation:

$$^3J_{(H,H)} = 13.7\cos^2\phi - 0.73\cos\phi + \Sigma i\Delta\chi_i[0.56 - 2.47\cos^2(z_i\phi + 16.9\,|\Delta\chi_i|)].$$

In this equation, ϕ is the dihedral angle between the two protons, z is the orientation factor of substituent i, $\Delta\chi_i$ is the electronegativity difference between substituent i and the respective proton. $\Delta\chi_c$ is calculated between the protons and the two other substituents bound to the same C-atom. Not only the direct substituents i_α are considered but also the atoms bonded to the i_α substituents (i_β). Thus, $\Delta\chi_i$ is determined according to:

$$\Delta\chi_i = \Delta\chi_{i,\alpha} - 0.14\Sigma\Delta\chi_{i,\beta}\ (O{:}\Delta\chi_i = 1.3,\ C{:}\Delta\chi_i = 0.4,\ H{:}\Delta c_i = 0).$$

The coupling constants are 11.63 Hz for $\phi = 180°$(*ap*), 3.55 Hz for 60° ((+)-*sc*) and 1.97 Hz for −60° ((−)-*sc*), respectively, for both C(2)H protons.

Compound	Repetition unit	Coupling constant	Coupling [Hz]	*ap* [%]	(−)-*sc* [%]	(+)-*sc* [%]
16-Mer	Bulk	^3J(C(2)H^{Si},C(3)H)	7.3	35.4	53.7	9.2
		^3J(C(2)H^{Re},C(3)H)	5.7			
	terminal residue 1	^3J(C(2)H^{Si},C(3)H)	6.4	50.3	45.1	4.6
		^3J(C(2)H^{Re},C(3)H)	6.9			
	terminal residue 2	^3J(C(2)H^{Si},C(3)H)	7.2	49.7	54.9	−4.6
		^3J(C(2)H^{Re},C(3)H)	6.7			
20-Mer	CH_2	^3J(C(2)H^{Si},C(3)H)	7.4	35.4	54.6	10
		^3J(C(2)H^{Re},C(3)H)	5.5			
	CHD	n.d.	n.d.	n.d.	n.d.	n.d.
		^3J(C(2)H^{Re},C(3)H)	5.6			

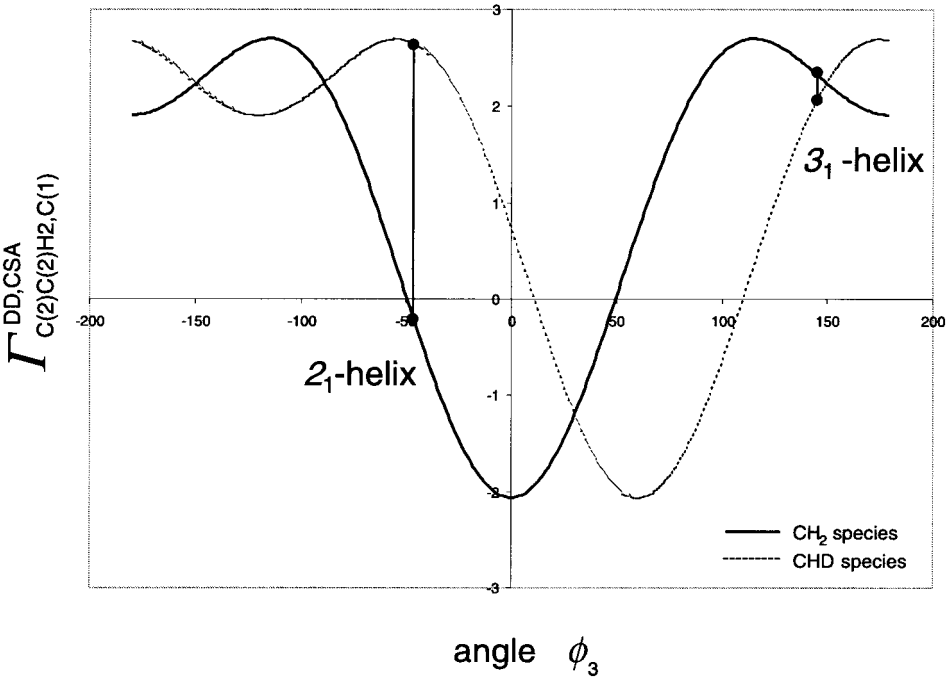

Fig. 8. *The dependence of* $\Gamma^{DD,CSA}_{C(2)C(2)H,C(1)}$ *on* ϕ_3. *Solid line:* CHD unit, *dashed line:* CH_2 unit. The theoretical values for a 3_1 and a 2_1 helix are indicated. The values on the *y*-axis are arbitrary.

The ZQ and the DQ spectra for the 16-mer are shown in *Fig. 9*. The $\Gamma^{DD,CSA}_{C(2)C(2)H,C(1)}$ values for the 16-mer bulk units are positive. In the 20-mer, the rates for the nondeuterated as well as for the deuterated unit are also positive, as can be inferred from the relative intensities of the *multiplet* components. This excludes the 2_1 helix as predominant conformation, whereas the 3_1 helix ($\phi_3 = 151°$) is still possible.

Conformational Analysis: ROE Data. – The design of the selectively labeled 20-mer **2** offers the opportunity to obtain unit-specific information due to the possibility of spectral editing for the multiplicity of CH_n groups using a $^{13}CH_x$-edited ROESY pulse sequence. Thus, the C(2)HD group can be separated from the $C(2)H_2$ group, and the different $C(4)H_nD_m$ isotopomers can be separated from each other. The goal of this experiment is a comparative analysis of cross-peak intensities of the two ^{13}C-labeled units in order to probe the presence of a 3_1-helix (*Table 3*).

Table 3. *Characteristic Interresidual H,H Distances in the* 2_1 (i, $i+2$ distances) *and the* 3_1*-Helix* (i, $i+3$).

	$i,i+2$-Distances [Å]		$i,i+3$-Distances [Å]	
	C(4)H	C(3)H	C(4)H	C(3)H
$C(2)H^{Re}$	3.2	5.2	5.3	4.6
$C(2)H^{Si}$	4.8	6.7	6.7	3.2

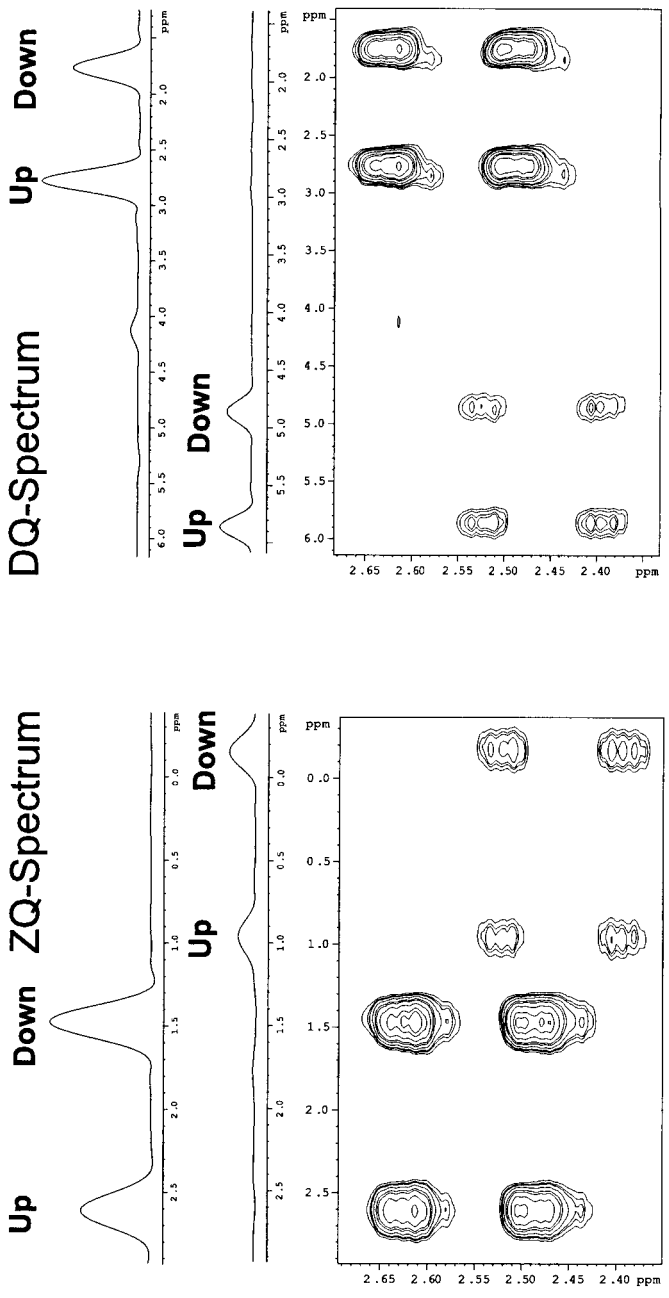

Fig. 9. J-*Coupled CT HCC-COSY experiment recorded with the 16-mer* **1** (T = $2/J_{(CC)}$). *Left:* ZQ experiment, *right:* DQ experiment. 1D Columns are extracted for the two *multiplets*, showing the different relaxation of the *multiplet* components. The more intense signal is the bulk signal, the other one belongs to the terminal 2 residue.

A schematic presentation of the different cross-peak patterns of these two units in the $^{13}CH_x$-edited ROESY spectrum is given in *Fig. 10*. The corresponding spectra recorded at 20° are shown in *Fig. 11*.

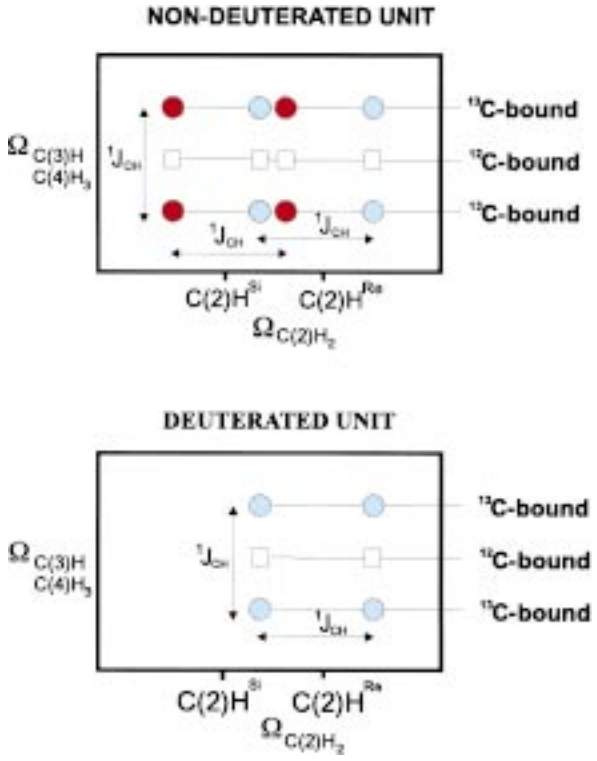

Fig. 10. *Scheme of the* multiplet *pattern of the C(2)H$_2$,C(3)H and the C(2)H$_2$,C(4)H$_3$ cross-peaks in the CH$_x$-filtered ROESY spectrum for the nondeuterated and the deuterated ^{13}C-labeled unit of the 20-mer* **2**. Corresponding regions of the CH$_x$-filtered ROESY spectra are shown in *Fig. 11*

Relative intensities of the interresidual ROE signals extracted from the CH$_x$-filtered ROESY spectra recorded at 20° and −27° are collected for both labeled units in *Table 4*. No significant difference in any cross-peak intensity was observed for C(2)H^{Si} and C(2)H^{Re} signals, hence, they can both be regarded as C(2)H$_2$. If either one of the helices would be the predominant conformation of the 20-mer, differential effects should be detectable between the two C(2)H$_2$ protons. All of the interresidual ROE signals appear between ^{13}C-labeled units and the ^{12}C units. No interresidual ROEs between the ^{13}C-labeled units were detected, although C(2)H$_2$ to C(2)H$_2i+3$ and C(4)H$_3i+3$ signals could potentially be resolved due to a primary or secondary isotope shift. However, neither of these ROE signals is to be expected in a 3_1 helix (all of these distances are 5.3 Å or larger). The indicative C(2)H$_2$,C(3)H$i+3$ cross-peak for a 3_1 helix cannot be resolved from the intraresidual cross-peak. However, signal-intensity differences between the nondeuterated and the deuterated units for this cross-peak have been observed. While there is a strong ^{13}C(2)H$_2$,^{12}C(3)H ROE for the

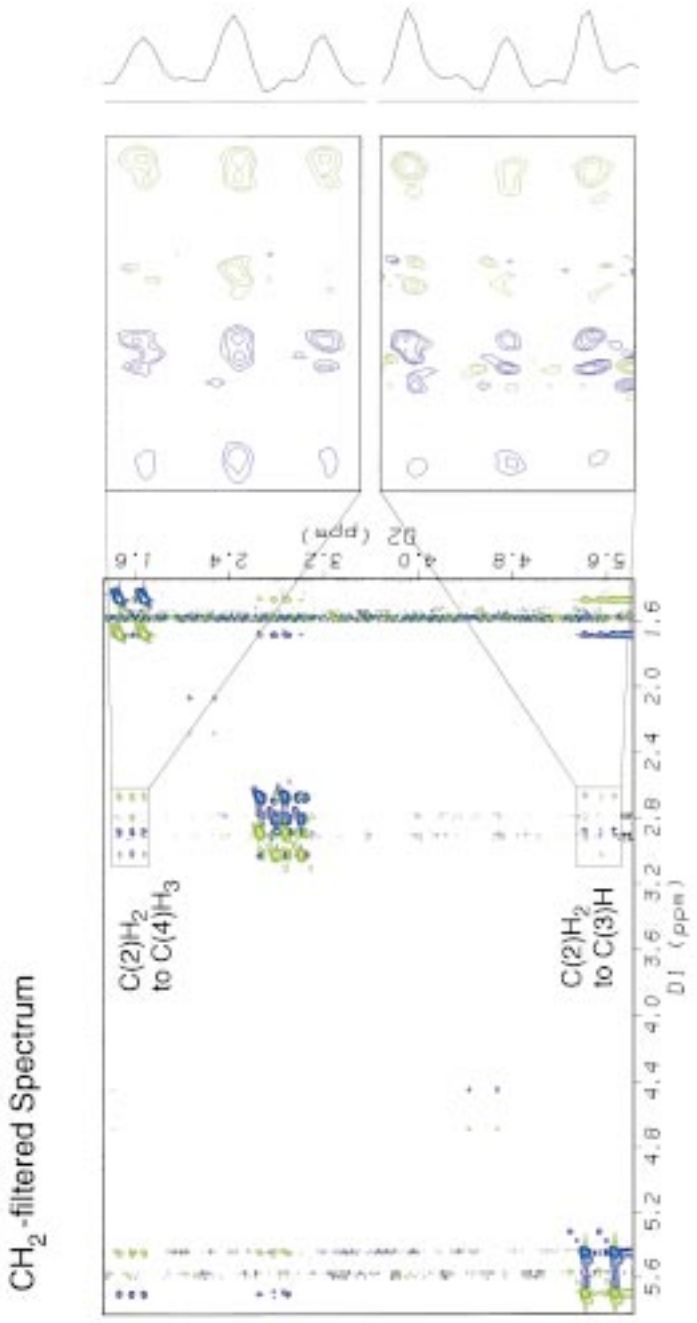
CH2-filtered Spectrum
C(2)H2 to C(4)H3
C(2)H2 to C(3)H
D2 (ppm)
D1 (ppm)

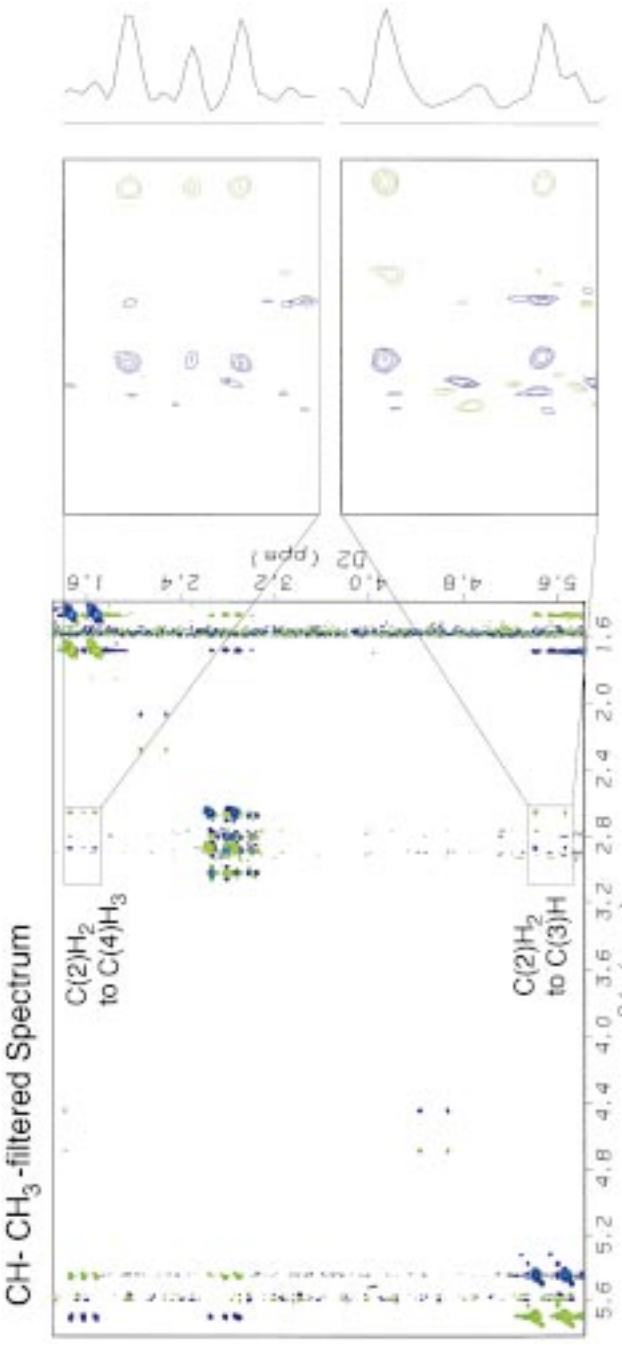

Fig. 11. *CH_x-Filtered ROESY spectra of the 20-mer* **2** *at 20° for the nondeuterated and the deuterated units.* $C(2)H_2$ to C(3)H and $C(4)H_3$ cross-peaks have been magnified, and 1D columns have been extracted.

Table 4. *Interresidual ROE Signals of the 20-Mer* **2** *from the CH_x-Filtered ROESY Spectra at 26° and at −30°.* Relative ROE intensities are indicated by the number of '+', n.d. = not determined.

	Proton-ID	Proton-ID	Signal intensity at	
			20°	−27°
Undeuterated unit	C(2)H	^{12}C(4)H	++	+++
	C(2)H	^{12}C(3)H	+	+++
	C(4)H	^{12}C(3)H	++	+++
	C(4)H	^{12}C(2)H	n.d.	n.d.
Deuterated unit	C(2)H^{Re}	^{12}C(4)H	+	+
	C(2)H^{Re}	^{12}C(3)H	−	+
	C(4)H	^{12}C(3)H	−	−

nondeuterated unit, the corresponding ^{13}C(2)H^{Re},^{12}C(3)H cross-peak is very weak for the deuterated unit (*Fig. 11*). Also, relative to the respective intraresidual ^{13}C(2)H$_2$,^{13}C(3)H signals, the signal of the deuterated unit is weaker than that of the nondeuterated one. In agreement with the presence of a 3_1 helix, this indicates that the deuterated unit shows a C(2)H$_2$,C(3)H$i+3$ contact to the undeuterated unit, while the nondeuterated unit shows the same contact to a ^{12}C unit. If a 3_1 helix were the predominant conformation, then only the two C(2)H$_2$,C(3)H cross-peaks would have to be of different intensity, since in this conformation the C(2)H^{Re},C(3)H$i+3$ distance is 4.6 Å while C(2)H^{Si} and C(3)H$i+3$ are only 3.2 Å apart from each other.

Conformational Analysis: Temperature Dependence. Some of the interresidual signals become more intense with decreasing temperature (*Table 4*), suggesting a less-averaged conformation at lower temperature. This is most pronounced for the C(2)H$_2$,C(3)H ROE in the nondeuterated unit. Also, the same ROE intensifies slightly in the nondeuterated unit. In contrast, the intensity of other interresidual signals does not change.

^{1}H-1D Spectra recorded at different temperatures (*Fig. 12*) show that $^3J_{(C(2)H,C(3)H)}$-coupling constants do not change significantly with temperature, which – in combination with the inconsistent temperature dependence of some ROE signals – leads us to assume that there can be no pronounced temperature dependence of the conformation.

4. Conclusions. – In conclusion, we synthesized and investigated the structures of two specifically labeled linear oligo(hydroxybutanoates) by NMR spectroscopy in solution. Due to similarity in $^3J_{(H,H)}$ and $^3J_{(C,H)}$-coupling constants, we conclude that both compounds adopt the same conformation. In these compounds, all but five to six terminal residues adopt the same conformation. The labeling scheme of the 20-mer made a unit-specific conformational analysis within the PHB chain possible. All acquired NMR parameters show that the conformation is averaged. According to the analysis of homonuclear $^3J_{(C(2)H,C(3)H)}$-coupling constants the structure of both compounds is strongly averaged, with neither of the helices contributing significantly to the conformational ensemble. Interresidual-distance information from ROE data confirms unit-specifically that the structure of the 20-mer is averaged, and that neither one of the two helices is the predominant conformation. The analysis of $\Gamma^{DD,CSA}_{C(2)C(2)H,C(1)}$

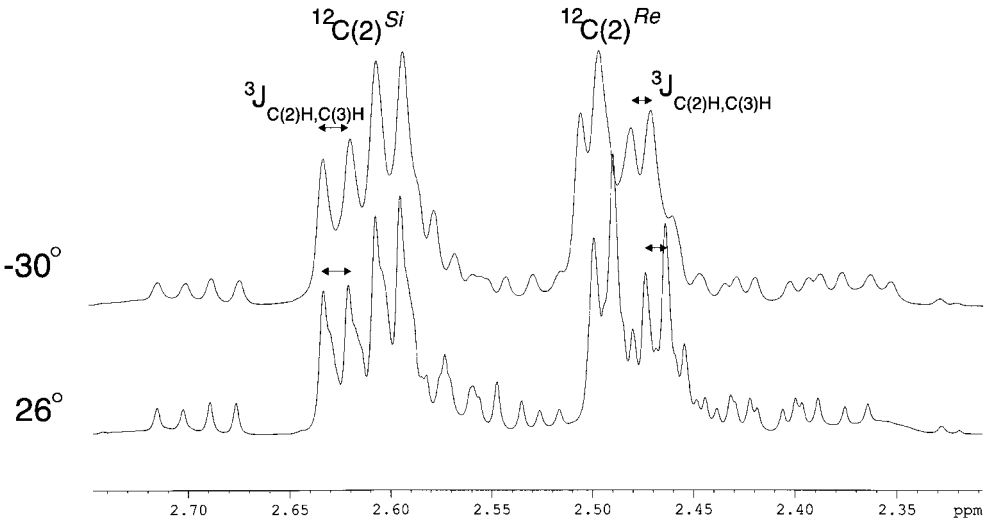

Fig. 12. *1D Spectra of the 20-mer* **2** *at 26° and at −30°*

excludes the 2_1 helix as the possible conformation. The averaged conformation is maintained even at temperatures as low as −30°. The extremely high flexibility of the PHB backbone on the NMR time scale is in line with conclusions about its biological role as ion-channel component and as appendage of proteins where it has never been structurally identified, for instance, by diffraction methods [9].

Experimental Part

General. Ethyl 3-oxobutanoate **3*** was purchased from *CAMPRO Scientific*, Germany. All other reagents were used as received from *Fluka* or *Senn*. All labeled compounds **1**–**2**, **4***–**7***, **9**, **10***, **11***, **13**, **14**, **16**–**18** were synthesized as described for the unlabeled isomers [11]. Compounds **6**, **7**, **10**, and **12** were prepared according to the procedure in [11]. IR Spectra: *Perkin-Elmer 1600-FT* spectrophotometer. ^{1}H-NMR: *Bruker AMX-II-500* (500 MHz), *AMX-400* (400 MHz), *ARX-300* (300 MHz), or *Varian Gem-200* (200 MHz) spectrometer. ^{13}C-NMR: *Bruker AMX-II-500* (125 MHz), *AMX-400* (100 MHz), *ARX-300* (75 MHz), or *Varian Gem-200* (50 MHz) spectrometer; in $CDCl_3$ unless other specified. All 2D measurements have been performed on *Bruker DRX-600* spectrometers in the *Francis Bitter Magnet Laboratory* and the *Department of Chemistry* at M.I.T. For both compounds, the experiments have been recorded using 10-mg samples in 500 ml $CDCl_3$. Different HC(C)H-E.COSY experiments [20] have been performed to obtain homo- and heteronuclear ^3J-coupling constants. For the deuterated 20-mer, a CH_x-edited ROESY was recorded to separate CH_n moieties, where n is either even or odd, resulting in a separation of ROE signals from the D-labeled and the unlabeled residue. To investigate the overall conformation of the 20-mer in $CDCl_3$ and the temp. dependence of the conformation, CH_x-filtered ROESY spectra were taken at 20° and −27°. All other experiments were carried out at 20°. MS: *VG ZAB2-SEQ* for LSI (FAB) with 3-nitrobenzyl alcohol as matrix; and *Bruker Reflex MALDI-TOF* spectrometer for MALDI-TOF.

*Ethyl (*R*)-3-Hydroxy[1,2,3,4-$^{13}C_4$]butanoate* (**4***). ^{1}H-NMR (300 MHz): 4.19 (*m*, $^1J(H,^{13}C) = 144.6$, C*H*OH); 4.18 (2*dq*, $^3J(H,H) = 7.2$, $^3J(H,^{13}C) = 3.3$, $J = 0.9$, MeCH_2); 3.03 (br. *s* OH); 2.45 (*m*, $^1J(^{13}C,H) = 127.2$, CH_2); 1.28 (*td*, $^3J(H,H) = 7.2$, $J = 0.9$, *Me*CH_2); 1.23 (*qd*, $^1J(^{13}C,H) = 141.9$, $^2J(^{13}C,H) = 141.9$, $^2J(^{13}C,H) = 5.1$, $^3J(^{13}C,H) = 0.9$, Me). ^{13}C-NMR (300 MHz): 173.25, (*ddd*, $J = 228.3$, 19.5, 9.9, C(4)); 64.40 (*t*, $J = 150.6$, C(3)); 60.78 (MeCH_2); 42.85 (*dd*, $J = 145.5$, 223.2, C(2)); 22.47 (*dd*, $J = 155.1$, 19.5, C(4)); 14.24 (*Me*CH_2).

*Benzyl (*R*)-3-[(*tert*-Butyl)diphenylsilyloxy][1,2,3,4-$^{13}C_4$]butanoate* (**5***). ^{1}H-NMR (300 MHz): 7.69–7.63 (*m*, Ph); 7.45–7.27 (*m*, Ph); 5.06 (*dd*, ^2J = 12.3, ^3J(H,^{13}C(1)) = 3.0, 1 H, PhCH_2); 4.99 (*dd*, ^2J = 12.3, ^3J(H,^{13}C(1)) = 3.0, 1 H, PhCH_2); 4.31 (*m*, ^1J(H,^{13}C(3)) = 145.5, CH); 2.60 (*d*, *J* = 4.2, ^1J(H,^{13}C(2)) = 130.5, CH); 2.44 (*m*, *J* = 3.3, ^1J(H,^{13}C(2)) = 127.8, CH); 1.10 (*qd*, *J* = 4.8, ^1J(H,^{13}C(4)) = 126.6, ^{13}C(4)H_3); 1.02 (*s*, *t*-Bu). ^{13}C-NMR (300 MHz): 171.54 (*dd*, ^1J(C(1),C(2)) = 228.3, ^2J = 9.9, C(1)); 145.45 (*dd*, *J* = 165.0, 281.8, PhCH_2); 136.17 (*d*, *J* = 9.9, PhSi); 134.36 (*d*, *J* = 92.1, PhSi); 129.88 (*d*, *J* = 24.3, PhSi); 128.79 (*s*, PhCH_2); 128.4 8 (*d*, *J* = 24.3, PhCH_2); 127.80 (*d*, *J* = 19.5, PhSi); 123.24 (*d*, *J* = 281.5, PhSi); 122.24 (*d*, *J* = 281.5, PhSi); 67.02 (*t*, ^1J(C(3),C(2)) = ^1J(C(3),C(4)) = 155.4, C(3)); 44.74 (*dd*, ^1J(C(2),C(3)) = 155.4, ^1J(C(2),C(1)) = 228.3, C(2)); 26.97 (*s*, Me_3C); 23.70 (*d*, ^1J(C(4),C(3)) = 155.4, C(4)); 18.34 (*d*, *J* = 33.9, PhSi); 17.79 (*d*, *J* = 29.1, PhSi).

*Benzyl (*R*)-3-Hydroxy-[1,2,3,4-$^{13}C_4$]butanoate* (**7***). ^{1}H-NMR (300 MHz): 7.73–7.66 (*m*, Ph); 7.48–7.32 (*m*, Bn); 5.15 (*d*, *J* = 3.3, PhCH_2); 4.21 (*m*, ^1J(^{13}C,H) = 144.9, *J* = 2.1, CH); 2.92 (*s*, OH); 2.50 (*m*, ^1J(^{13}C,H) = 130.5, *J* = 3.0, *J* = 1.5, CH_2); 1.22 (*qd*, ^1J(^{13}C,H) = 126.0, *J* = 4.5, 3 H, *Me*CH); 1.09 (*d*, *J* = 1.2, *t*-Bu). ^{13}C-NMR (300 MHz): 173.04 (*dd*, *J* = 19.5, ^1J = 233.2, C(1)); 146–122 (PhCH_2, PhSi); 64.41 (*t*, ^1J(C(3),C(4)) = 155.4, C(3)); 42.90 (*dd*, ^1J = 150.6, ^1J = 228.3, C(2)); 26.0 (*s*, Me_3C); 22.49 (*dd*, ^1J(C(4),C(3)) = 155.4, *J* = 19.5, C(4)); 18.30 (*d*, *J* = 33.9, PhSi); 17.75 (*d*, *J* = 29.1, PhSi).

*(*R*)-3-[(*tert*-Butyl)diphenylsilyloxy][1,2,3,4-$^{13}C_4$]butanoic Acid* (**6***). ^{1}H-NMR (300 MHz): 7.70–7.65 (*m*, Ph); 7.46–7.33 (*m*, Ph); 4.26 (*dm*, ^1J(^{13}C,H) = 145.8, H–C(3)); 2.52 (*m*, ^1J(^{13}C,H) = 130.2, *J* = 4.8, *J* = 5.4, 1 H, CH_2); 2.46 (*m*, ^1J(^{13}C,H) = 127.8, 1 H, CH_2); 1.13 (*qd*, ^1J(^{13}C,H) = 126.3, *J* = 4.8, *J* = 5.4, 3 H-C(4)); 1.03 (*s*, *t*-Bu). ^{13}C-NMR (300 MHz); 177.23 (*dd*, ^1J(C(1),C(2)) = 213.7, *J* = 9.6, C(1)); 136.02 (*s*, PhSi); 133.86 (*d*, *J* = 150.34, PhSi); 129.90 (*d*, *J* = 29.1, PhSi); 127.78 (*d*, *J* = 24.0, PhSi); 66.84 (*t*, ^1J(C(3),C(4)) = ^1J(C(3),C(2)) = 150.6, C(3)); 44.26 (*dd*, ^1J(C(2),C(3)) = 150.6, ^1J(C(2),C(1) = 213.7, C(2)); 35.13 (*dd*, *J* = 135.6, *J* = 218.2, PhSi); 27.03 (*s*, PhSi); 23.54 (*d*, *J* = 155.4, C(4)); 18.62 (*dd*, *J* = 155, 296.2, PhSi); 13.78 (*dd*, *J* = 14.4, 135.9, PhSi).

*(2*R*)-5-Bromo-6-(bromo[$^{13}C_1$]methyl)-2-(*tert*-butyl)-4-oxo[4,5,6-$^{13}C_3$]-[1,3,5]-dioxin* (**8**). IR ($CHCl_3$): 2981*m*, 2967*m*, 2910*w*, 2876*w*, 1702*s*, 1547*s*, 1484*m*, 1463*w*, 1418*w*, 1406*m*, 1370*m*, 1308*s*, 1275*w*, 1154*m*, 1121*m*, 1074*s*, 1048*w*, 988*w*, 962*m*, 926*w*. ^{1}H-NMR (300.08 MHz): 5.16 (*t*, ^3J(H,C) = 1.8, H–C(2)); 4.30 (*dddd*, *J* = 157.5, 10.8, 2.7, 1.8, 1 H, BrCH_2); 4.09 (*dddd*, *J* = 154.8, 10.8, 5.7, 4.8, 1 H, BrCH_2); 1.08 (*s*, *t*-Bu). ^{13}C-NMR (300.06 MHz): 166.09 (*dd*, *J* = 335.2, 233.2, C(4)); 158.92 (*d*, *J* = 310.6, C(5)); 107.55 (*s*, C(2)); 93.94 (*ddd*, *J* = 330.1, 310.6, 19.5, C(6)); 34.66 (*s*, Me); 25.39 (*ddd*, *J* = 228.0, 19.2, 9.6, Br^{13}CH_2); 23.90 (*s*, Me_3C). EI-MS 336.0 (1.0), 335.0 (4.7), 334.0 (15.7), 332.0 (9.0), 332.0 (29.6), 331.0 (4.9), 330.0 (14.9), 290.0 (3.2), 288.9 (5.9), 286.9 (3.1), 255.0 (1.2), 254.1 (3.0), 253.1 (2.2), 252.1 (3.0), 251.0 (2.2), 249.9 (1.6), 248.9 (37.6), 247.9 (50.6), 246.9 (77.5), 245.9 (100), 244.9 (40.1), 243.9 (50.4), 242.9 (1.7), 238.0 (12.9), 237.0 (1.0), 236.0 (12.4), 219.9 (2.2), 217.9 (4.7), 215.9 (2.3), 196.0 (4.0), 194.0 (3.8), 176.9 (4.1), 174.9 (8.4), 172.9 (4.5), 169.0 (8.3), 168.0 (23.3), 167.0 (10.3), 166.0 (23.8), 165.0 (1.7), 151.9 (23.5), 149.9 (24.6), 149.0 (1.1), 138.0 (4.3), 136.0 (4.2), 124.9 (3.6), 123.9 (4.5), 122.9 (4.6), 121.9 (6.4), 109.0 (7.4), 107.0 (7.4), 87.1 (2.7), 86.1 (15.4), 85.1 (4.6), 71.1 (3.8), 69.1 (3.7), 57.1 (17.5), 41.1 (2.1).

*Benzyl (2*S*,3*R*)-[1,2,3,4-$^{13}C_4$,2,4-$^2H_2$]butanoate* (**9**). IR ($CHCl_3$): 3672*w*, 3539*m*, 3081*w*, 3067*w*, 2962*m*, 2889*w*, 2454*w*, 2212*w*, 1951*w*, 1873*w*, 1810*w*, 1678*s*, 1604*w*, 1498*m*, 1455*m*, 1375*m*, 1299*m*, 1265*m*, 1160*s*, 1080*m*, 1018*m*, 914*m*, 820*w*. ^{1}H-NMR (300.08 MHz): 5.16 (*d*, ^2J = 3.3, PhCH_2); 4.21 (*m*, ^1J = 143.7, H–C(3)); 2.89 (*s*, OH); 2.52 (*m*, ^1J = 126.6, *J* = 2.7, H–C(2)); 1.22 (*m*, ^1J = 126.0, 2 H–C(4)). ^{13}C-NMR (300.08 MHz): 172.90 (*dd*, *J* = 223.3, 19.5, C(1)); 135.74; 128.83; 128.60; 128.46; 66.67; 64.34 (*t*, *J* = 150.3, C(3)); 42.61 (*ddt*, *J* = 155.4, 77.7, 155.4, C(2)); 22.57–21.77 (*dd*, *dq*, *dh*, ^2J = 19.5, *J* = 160.2, *J* = 77.7, *J* = 77.7, C(4)). D-NMR (400 MHz): 2.477 (*d*, *J* = 128.8, D–C(2)); 1.217 (*d*, *J* = 125.8, D–C(4)). EI-MS: 203.2 (2.2), 202.2 (5.7), 201.2 (8.7), 200.1 (7.3), 199.1 (3.1), 181.1 (4.0), 173.2 (2.4), 172.2 (5.9), 171.1 (6.9), 170.1 (4.3), 155.1 (3.1), 154.1 (6.1), 152.1 (5.0), 110.1 (1.9), 109.1 (8.3), 108.1 (60.5), 107.1 (52.2), 106.1 (9.7), 105.1 (24.4), 93.1 (2.1), 92.1 (11.6), 91.1 (100), 90.1 (7.8), 89.1 (4.7), 79.1 (7.8), 78.1 (2.2), 77.1 (5.8), 65.1 (4.3).

*α-Benzyl-ω-[(*tert*-butyl)diphenylsilyloxy]bis[(*R*)-oxy(3-[$^{13}C_1$]methyl-1-oxo[1,2,3-$^{13}C_3$]propane-1,3-diyl]* (**10***). ^{1}H-NMR (300 MHz): 7.70–7.63 (*m*, Ph); 7.42–7.30 (*m*, Ph); 5.22 (*d*, ^1J(H–C(3),CH) = 151.5, *J* = 2.4, CH); 5.08 (*d*, *J* = 3.0, PhCH_2); 4.24 (*d*, ^1J(H,C(3)) = 145.5, *J* = 3.3, CH); 2.64 (*d*, ^1J(H,C(2)) = 130.5, 1 H, CH_2); 2.51 (*d*, ^1J(H,C(2)) = 128.7, 1 H, CH_2); 2.45 (*d*, ^1J(H,C(2)) = 129.6, 1 H, CH_2); 2.32 (*d*, ^1J(H,C(2)) = 128.7, 1 H, CH_2); 1.22 (*qdd*, ^1JH,C(4)) = 127.2, *J* = 4.8, *J* = 1.5, C(4)H_3); 1.09 (*qdd*, ^1J(H,C(4)) = 126.0, *J* = 4.8, *J* = 1.5, C(4)H_3); 1.03 (*s*, *t*-Bu). ^{13}C-NMR (300 MHz): 170.70 (*d*, ^1J(C(1),C(2)) = 228.0, C(1)); 170.33 (*dd*, ^1J(C(1),C(2)) = 228.0, *J* = 9.6, C(1)); 136.10 (*d*, *J* = 9.6, PhSi); 134.39 (*d*, *J* = 97.2, PhSi); 129.89 (*d*, *J* = 19.5, PhSi); 128.84 (*s*, PhSi); 128.55 (*d*, *J* = 9.9, PhSi); 127.80 (*d*, *J* = 19.5, PhSi); 67.39 (*t*, ^1J(C(3),C(2) = ^1J(C(3),C(4)) = 160.2, C(3)); 66.85 (*t*, ^1J(C(3),C(2)) = ^1J(C(3),C(4)) = 160.2, C(3)); 44.71 (*dd*, *J* = 155.4, 228.3, C(2)); 40.82 (*dd*, *J* = 155.4, 228.3, C(2)); 26.98 (*s*, PhSi); 23.44 (*d*, ^1JCH,C(4)) = 155.4, C(4)); 19.83 (*dd*, ^1J(H,C(4)) = 155.4, ^2J(C(4),H) = 9.6, C(4)).

*α-Hydroxy-ω-[(*tert*-butyl)diphenylsilyloxy]bis[(*R*)-oxy(3-[$^{13}C_1$]methyl-1-oxo[1,2,3-$^{13}C_3$]propane-1,3-diyl]* (**11***). ^{1}H-NMR (300.08 MHz): 7.68–7.66 (*m*, Ph); 7.45–7.34 (*m*, Ph); 5.18 (*m*, ^1J = 151.2, C*H*CH$_2$COOH); 4.24 (*m*, ^1J = 144.9, SiOCH); 2.70–2.27 (*m*, CH$_2$); 1.38 (*m*, ^1J = 39.6, *J* = 4.2, Me); 1.03 (*s*, *t*-Bu); 0.95 (*m*, ^1J = 41.1, *J* = 4.2, SiOCHMe). ^{13}C-NMR (300.08 MHz): 176.20 (*d*, ^1J = 223.2, COO); 170.69 (*d*, ^1J = 228.1, COO); 135; 134.38; 134.00; 129.84; 129.76; 127.75; 127.67; 67.38 (*t*, *J* = 77.2, OCH); 66.86 (*t*, *J* = 77.7, OCH); 44.77 (*dd*, ^1J = 228.4, *J* = 155.4, *C*H$_2$COOH); 40.52 (*dd*, ^1J = 223.3, *J* = 160.2, SiOCH*C*H$_2$); 27.05; 23.54 (*d*, ^1J = 155.4, CH$_3$); 19.91 (*d*, ^1J = 155.1, SiOCHMe).

*α-Benzyl-ω-[(*tert*-butyl)diphenylsilyloxy][bis[(*R*)-oxy(3-methyl-1-oxopropane-1,3-diyl)]bis[(*R*)-oxy(3-[$^{13}C_1$]methyl-1-oxo[1,2,3-$^{13}C_3$]propane-1,3-diyl)]]* (**13**). Ir (CHCl$_3$): 3072*m*, 2864*m*, 2932*m*, 2858*m*, 1959*w*, 1895*w*, 1736*s*, 1690*s*, 1587*w*, 1456*m*, 1427*m*, 1382*m*, 1368*m*, 1301*m*, 1290*m*, 1176*s*, 1110*s*, 1106*s*, 1060*s*, 994*m*, 910*w*, 822*m*, 613*m*. ^{1}H-NMR (300.06 MHz): 7.69–7.63 (*m*, Ph); 7.45–7.28 (*m*, Ph); 5.29 (*m*, *J* = 6.6, *J* = 1.8, CH); 5.21 (*m*, CH); 5.18 (*m*, ^1J = 151.2, *J* = 2.4, ^{13}CH); 5.12 (*s*, PhCH$_2$); 4.26 (*m*, ^1J = 145.2, *J* = 3.0, SiOCH); 2.68 (*dd*, ^2J = 15.6, ^3J = 7.5, 1 H, *H*^{Re}CH); 2.53 (*dd*, ^2J = 15.6, ^3J = 5.4, 1 H, HC*H*^{Si}); 2.52 (*dd*, ^2J = 15.6, ^3J = 7.5, 1 H, *H*^{Re}CH); 2.37 (*dd*, ^2J = 15.6, ^3J = 6.3, HC*H*^{Si}); 2.85–2.09 (*m*, ^{13}CH$_2$); 1.27 (*d*, ^3J = 6.3, Me); 1.21 (*dm*, ^1J = 127.2, *J* = 4.5, ^{13}CH$_3$); 1.21 (*d*, ^3J = 6.3, Me); 1.11 (*m*, ^1J = 126.3, ^{13}CH$_3$); 1.03 (*s*, *t*-Bu). ^{13}C-NMR (300.06 MHz): 170.50 (*d*, ^1J = 228.3, ^{13}COO); 169.37 (*dd*, ^1J = 228.3, ^3J = 9.6, SiOCHCH$_2$*C*OO); 136.00; 135.87; 134.43; 134.10; 129.82; 129.76; 128.77; 128.53; 127.75; 127.67; 67.38 (*t*, ^1J = 140.7, O^{13}CH); 66.86 (*t*, ^1J = 145.8, SiOCH); 44.74 (*dd*, ^1J = 228.0, ^2J = 155.1, ^{13}CH$_2$); 41.03 (*dd*, ^1J = 233.1, ^2J = 160.2, SiOCH*C*H$_2$); 27.08; 23.59 (*d*, ^1J = 155.4, ^{13}CH$_3$); 20.00; 19.90 (*d*, ^1J = 155.1, SiOCH*Me*); 19.90. MALDI-TOF-MS: 717.6 (0.91), 720.6 (2.9), 721.6 (55.28), 722.6 (24.97), 723.6 (11.58), 724.7 (3.52), 725.6 (0.79).

*α-Benzyl-ω-[(*tert*-butyl)diphenylsilyloxy]bis{bis[(*R*)-oxy(3-methyl-1-oxopropane-1,3-diyl)]bis[(*R*)-oxy(3-[$^{13}C_1$]methyl-1-oxo[1,2,3-$^{13}C_3$]propane-1,3-diyl)]}* (**14**). IR (CHCl$_3$): 3011*m*, 2969*m*, 2932*m*, 2859*m*, 1736*s*, 1690*s*, 1456*m*, 1428*m*, 1383*m*, 1369*m*, 1299*m*, 1290*m*, 1173*s*, 1105*s*, 1159*s*, 1037*w*, 993*m*, 976*m*, 8.22*m*. ^{1}H-NMR (300.06 MHz): 7.68–7.65 (*m*, Ph); 7.45–7.30 (*m*, Ph); 5.24 (*m*, ^1J = 151.5, *J* = 3.9, 2, ^{13}CH); 5.36–5.16 (*m*, *J* = 6.3, 4 CH); 5.18 (*m*, ^1J = 151.5, 1 ^{13}CH); 5.12 (*s*, PhCH$_2$); 4.25 (*m*, ^1J = 145.5, SiOCH); 2.88–2.09 (*m*, ^{13}CH$_2$); 2.72–2.36 (*m*, CH$_2$); 1.28 (*m*, ^1J = 127.2, ^{13}CH$_3$); 1.21 (*m*, ^1J = 127.2, 1 ^{13}CH$_3$); 1.11 (*m*, ^1J = 126.3, SiOCH*Me*); 1.28 (*d*, ^3J = 6.0, 1 Me); 1.26 (*d*, ^3J = 6.0, 2 Me); 1.24 (*d*, ^3J = 5.7, 1 Me); 1.03 (*s*, *t*-Bu). ^{13}C-NMR (300.06 MHz): 170.47 (*d*, ^1J = 233.1, ^{13}COO); 169.3 (*d*, ^1J = 228.0, 2 ^{13}COO); 169.29 (*d*, ^1J = 233.1, 1 ^{13}COO); 169.29 (COO); 136.00; 134.45; 134.12; 129.84; 129.76; 128.77; 128.51; 127.75; 127.69; 67.77 (*t*, ^1J = 160.2, 2 O^{13}CH); 67.35 (*t*, ^1J = 150.3, 1 O^{13}CH); 66.88 (*t*, ^1J = 155.4, SiOC); 44.75 (*dd*, ^1J = 228.0, ^1J = 155.1, 1 ^{13}CH$_2$); 41.03 (*dd*, ^1J = 228.3, ^1J = 155.4, 1 ^{13}CH$_2$); 40.96 (*dd*, ^1J = 2 ^{13}CH$_2$); 27.10; 23.59 (*d*, ^1J = 155.4, ^{13}CH$_3$); 19.91 (*d*, ^1J = 155.1, 3 ^{13}CH$_3$); 19.95; 19.35. MS (MALDI): 1047.5, 1048.5 (5.51), 1049.5 (30), 1050.1 (7.09), 1051.1 (100.00), 1052.0 (53.44), 1053.1 (30.4), 1054.0 (11.1), 1055.0 (3.60).

*α-Benzyl-ω-[(*tert*-butyl)diphenylsilyloxy]tetrakis{bis[(*R*)-oxy(3-methyl-1-oxopropane-1,3-diyl)]bis[(*R*)-oxy(3-[$^{13}C_1$]methyl-1-oxo[1,2,3-$^{13}C_3$]propane-1,3-diyl)]}* (**1**). IR (CHCl$_3$): 2978*m*, 2933*m*, 1736*s*, 1692*s*, 1456*m*, 1427*m*, 1383*m*, 1370*m*, 1301*m*, 1291*s*, 1169*s*, 1104*m*, 1058*m*, 971*m*, 823*w*. ^{1}H-NMR (500.13 MHz): 7.68–7.65 (*m*, Ph); 7.42–7.34 (*m*, Ph); 5.25 (*m*, ^1J = 152.8, ^{13}CH); 5.33–5.21 (*m*, CH); 5.18 (*m*, ^1J = 152.7, 1 ^{13}CH); 5.12 (*s*, PhC*H*$_2$); 4.26 (*m*, ^1J = 145.3, SiOCH); 2.73–2.31 (*m*, ^{13}CH$_2$); 2.68–2.40 (*m*, CH$_2$); 1.27 (*m*, ^1J = 127.5, *J* = 4.1, ^{13}CH$_3$); 1.281 (*d*, ^3J = 6.2, 1 Me); 1.27 (*d*, ^3J = 6.3, Me); 1.26 (*d*, ^3J = 6.3, Me); 1.245 (*d*, ^3J = 6.3, 1 Me); 1.243 (*d*, ^3J = 6.3, 1 Me); 1.21 (*m*, ^1J = 127.4, *J* = 4.5, ^{13}CH$_3$); 1.11 (*m*, ^1J = 126.2, *J* = 4.5, SiOCH*Me*); 1.03 (*s*, *t*-Bu). ^{13}C-NMR (500 MHz): 170.30 (*d*, ^1J = 228.5, ^{13}COO); 169.90 (COO); 169.19 (*dd*, *J* = 230.5, 10.5, ^{13}COO); 169.17 (COO); 169.14 (COO); 169.14 (*dd*, *J* = 231.5, 8.5, ^{13}COO); 169.13 (COO); 135.83; 135.81; 135.72; 134.28; 133.94; 129.66; 129.59; 128.60; 128.35; 128.345; 127.59; 127.51; 67.60 (*t*, ^1J = 157.1, 67.76; 67.70; 67.17 (*td*, ^1J = 156.6, *J* = 8.7, O^{13}CH); 66.70 (*t*, ^1J = 155.5, O^{13}CH); 66.48; 44.58 (*dd*, ^1J = 228.4, ^1J = 154.5, ^{13}CH$_2$); 41.03 (Me); 40.86 (*ddd*, ^1J = 231.1, ^1J = 157.0, ^2J = 5.9, ^{13}CH$_2$); 40.78 (*dd*, ^1J = 231.5, *J* = 157.3, ^{13}CH$_3$); 40.64 (Me); 40.56 (Me); 27.0; 23.41 (*ddd*, ^1J = 155.7, ^2J = 8.4, ^3J = 4.6, ^{13}CH$_3$); 19.81 (Me). MALDI-TOF-MS: 1751.4 (3.6), 1752.4 (2.7), 1753.3 (3.0), 1754.3 (19.3), 1755.3 (100.00), 1756.3 (67.5), 1757.3 (49.7), 1758.3 (23.0), 1759.3 (12.0), 1760.3 (3.3).

*α-Benzyl-ω-[(*tert*-butyl)diphenylsilyloxy][[(*R*)-oxy(3-($^{13}C_1$)methyl-1-oxo[1,2,3-$^{13}C_3$]propane-1,3-diyl)]-bis[(*R*)-oxy(3-methyl-1-oxopropane-1,3-diyl)]]* (**16**). ^{1}H-NMR (300.08 MHz): 7.69–7.65 (*m*, Ph); 7.45–7.29 (*m*, Ph); 5.27 (*m*, *J* = 148.2, OC*H*CH$_2$CO$_2$Bn); 5.15 (*m*, *J* = 6.3, CH); 5.11 (*d*, *J* = 3.6, PhCH$_2$); 4.26 (*m*, *J* = 6.3, SiOCH); 2.65 (*m*, *J* = 130.2, C*H*^{Re}HCOOBn); 2.51 (*m*, *J* = 128.4, *J* = 3.3, CH*H*^{Si}COOBn); 2.53 (*dd*, ^2J = 6.9, ^3J = 5.1, C*H*^{Re}H); 2.48 (*dd*, ^2J = 6.9, ^3J = 3.0, CH*H*^{Si}); 2.38 (*dd*, ^2J = 6.6, C*H*^{Re}H); 2.33 (*dd*, ^2J = 6.9, ^3J = 3.6, CH*H*^{Si}); 1.24 (*m*, *J* = 127.5, 1,5, Me); 1.19 (*d*, *J* = 6.3, Me); 1.11 (*d*, *J* = 5.7, SiOCH*Me*); 1.03 (*s*, *t*-Bu). ^{13}C-NMR (300.08 MHz): 170.10 (*dd*, *J* = 232.9, 9.9, COOBn); 135.99; 134.12; 129.85; 129.78; 128.78; 128.55; 127.78; 127.69;

67.77 (*t*, *J* = 160.2, *C*HCH$_2$COOBn); 44.78; 41.06; 40.83 (*dd*, *J* = 232.9, 160.2, CH$_2$); 27.08; 23.62; 19.99 (*dd*, *J* = 155.4, 9.9, *Me*CHCH$_2$COOBn).

*α-Benzyl-ω-[(*tert*-butyl)diphenylsilyloxy]{octakis[(*R*)-oxy(3-methyl-1-oxopropane-1,3-diyl)]}{(*R*)-oxy(3-[$^{13}C_1$]methyl-1-oxo[1,2,3-$^{13}C_3$]propane-1,3-diyl)}bis[(*R*)-oxy(3-methyl-1-oxopropane-1,3-diyl)]}* (**18**). IR (CHCl$_3$): 2984*m*, 2934*m*, 2859*w*, 1738*s*, 1693*m*, 1457*m*, 1427*m*, 1382*m*, 1304*m*, 1265*m*, 1178*s*, 1134*m*, 1103*m*, 1083*m*, 1058*m*, 1005*m*, 997*m*, 976*m*, 822*w*, 612*w*. ^{1}H-NMR (300.08 MHz): 7.69 – 7.65 (*m*, Ph); 7.45 – 7.30 (*m*, Ph); 5.24 (*m*, *J* = 150.6, ^{13}CH); 5.25 (*m*, *J* = 6.0, *J* = OCH); 5.18 (*m*, *J* = 6.6, COC*H*); 5.12 (*s*, C*H*$_2$Ph); 4.25 (*m*, *J* = 6.3, SiOCH); 2.6 (*m*, ^{13}C*H*^{Re}H^{13}COO); 2.5 (*m*, ^{13}CH*H*^{Si}^{13}COO); 2.68 – 2.35 (*m*, CH$_2$); 1.24 (*m*, *J* = 127.5, 3 H, ^{13}CH$_3$); 1.28 (*d*, *J* = 6.0, 3 H, CH$_3$); 1.26 (*d*, *J* = 6.6, 18 H, 6 CH$_3$); 1.24 (*d*, *J* = 6.6, CH$_3$); 1.21 (*d*, *J* = 6.6, CH$_3$); 1.11 (*d*, *J* = 6.0, CH$_3$); 1.03 (*s*, 9 H, *t*-Bu). ^{13}C-NMR (300.08 MHz): 170.50; 170.10; 169.32; 169.31 (*dd*, *J* = 228.4, *j* = 9.9, ^{13}COO); 135.99; 135.86; 134.43; 134.09; 129.85; 129.77; 128.78; 128.54; 127.76; 127.68; 67.75; 67.69 (*dt*, *J* = 155.1, *J* = 19.5, O^{13}CH); 44.76; 40.96 (*s*, CH$_2$); 40.94 (*dd*, *J* = 232.9, *J* = 155.1, ^{13}CH$_2$); 27.08; 23.58; 19.93; 19.92 (*d*, *J* = 160.2, ^{13}CH$_3$); 19.33. MALDI-MS: 1320 (M^+), 1336 ([*M* + Na]$^+$), 1360 [*M* + Na + K]$^+$), 1229 [*M* – Bn]$^+$), 1143, 1057, 977, 971, 891, 885, 801, 715, 660, 629, 543, 440, 410, 367, 273.

*α-Benzyl-ω-[(*tert*-butyl)diphenylsilyloxy]{[(2*S*,3*R*)-oxy(3-([$^{13}C_1$,$^2H_1$]methyl-1-oxo-[1,2,3-$^{13}C_3$,2-$^2H_1$]propane-1,3-diyl)]octakis[(*R*)-oxy(3-methyl-1-oxopropane-1,3-diyl)]}* (**17**). IR (CHCl$_3$): 307*w*, 2985*m*, 2935*m*, 2858*w*, 1738*s*, 1694*m*, 1457*m*, 1427*m*, 1382*m*, 1305*m*, 1263*m*, 1178*s*, 1136*m*, 1103*m*, 1082*m*, 1059*m*, 1006*m*, 998*m*, 978*m*, 823*w*, 612*w*. ^{1}H-NMR (300.08 MHz): 7.68 – 7.65 (*m*, Ph); 7.44 – 7.31 (*m*, Ph); 5.28 (*m*, ^1J = 151.2, C*H*CDHCOO); 5.24 – 5.19 (*m*, *J* = 6.9, CH); 5.12 (*d*, ^2J = 3.0, PhCH$_2$); 4.25 (*m*, *J* = 6.3, SiOCH); 2.53 (*m*, ^1J = 128.7, CHDCOO); 2.62 – 2.34 (*m*, CH$_2$); 1.26 (*m*, ^1J = 127.5, C*H*$_{0;1;2;3}$D$_{0;1;2;3}$CHCHDCOO); 1.26 (*d*, *J* = 6.6, 5 Me); 1.24 (*d*, *J* = 6.3, Me); 1.21 (*d*, *J* = 6.6, Me); 1.11 (*d*, *J* = 6.0, SiOCH*Me*); 1.03 (*s*, *t*-Bu). ^{13}C-NMR (300.08 MHz): 170.11 (*dd*, *J* = 228.1, 9.6, COOBn); 169.39; 169.34; 136.00; 134.43; 134.09; 129.85; 129.77; 128.78; 128.54; 127.76; 127.68; 67.77 (*t*, *J* = 160.2, O*C*HCHDCOOBn); 66.88; 66.67; 66.64; 44.76; 41.04; 40.96; 40.51 (*ddt*, *J* = 77.4, 155.1, 77.4, *C*HDCOOBn); 27.06; 23.60; 20.09 – 19.15 (*dd*, *dt*, *dq*, *J* = 9.6, *J* = 77.7, CH$_{0;1;2;3}$D$_{0;1;2;3}$). D-NMR (400 MHz): 2.672 (*d*, *J* = 129.1, CHDCOOH); 1.275 (*d*, *J* = 125.7, CH$_2$D). MALDI-MS: 1166 ([*M* + Na + K]$^+$), 1151 ([*M* + Na]$^+$), 1057, 981 ([*M* – 2 HBn]$^+$), 881, 807, 795, 709, 623, 549, 453, 410, 367, 281, 273.

*α-Benzyl-ω-[(*tert*-butyl)diphenylsilyloxy]{octakis[(*R*)-oxy(3-methyl-1-oxopropane-1,3-diyl)]}{(*R*)-oxy(3-[$^{13}C_1$]methyl-1-oxo[1,2,3-$^{13}C_3$]propane-1,3-diyl)}bis[(*R*)-oxy(3-methyl-1-oxopropane-1,3-diyl)]{(2*S*,3*R*)-oxy(3-[$^{13}C_1$,$^2H_{0;1;2;3}$]methyl-1-oxo[1,2,3-$^{13}C_3$,2-$^2H_1$]propane-1,3-diyl)}octakis[(*R*)-oxy(3-methyl-1-oxopropane-1,3-diyl)]}* (**2**). IR (CHCl$_3$): 2985*m*, 2936*m*, 2859*w*, 1736*s*, 1693*m*, 1603*w*, 1457*m*, 1449*m*, 1427*m*, 1383*m*, 1305*s*, 1265*m*, 1178*s*, 1135*m*, 1102*m*, 1083*m*, 1059*s*, 1005*w*, 997*m*, 929*w*, 900*w*, 822*w*. ^{1}H-NMR (300.08 MHz): 7.68 – 7.65 (*m*, Ph); 7.42 – 7.34 (*m*, Ph); 5.24 (*m*, ^1J = 152.4, O^{13}CH); 5.25 (*m*, *J* = 6.6, 0.9, CH); 5.16 (*m*, *J* = 6.0, CH); 5.12 (*s*, PhCH$_2$); 4.25 (*m*, *J* = 6.3, SiOCH); 2.80 – 2.24 (*m*, ^{13}CH$_2$); 2.68 – 2.35 (*m*, CH$_2$, CDHCOO); 1.26 (*dm*, ^1J = 127.5, 2 ^{13}CH$_3$); 1.27 (*d*, ^3J = 6.0, Me); 1.267 (*d*, ^3J = 6.3, Me, CH$_{0;1;2;3}$D$_{0;1;2;3}$); 1.23 (*d*, ^3J = 7.2, Me); 1.21 (*d*, ^3J = 6.6, Me); 1.10 (*d*, ^3J = 5.7, SiOCHMe); 1.02 (*s*, *t*-Bu). ^{13}C-NMR (300.08 MHz): 170.50; 170.10; 169.34; 169.34 (*dd*, *J* = 233.2, 9.6); 135.98; 135.86; 134.43; 134.09; 129.85; 129.77; 128.78; 128.54; 127.76; 127.68; 67.77 (*t*, *J* = 155.4); 44.76; 40.94 (*dd*, *J* = 232.9, 160.2); 40.96; 40.63 (*m*, *J* = 77.7); 27.06; 23.60; 19.94; 19.93 (*dd*, *J* = 155.4, 9.6); 19.93 – 18.60 (*m*, *J* = 82.5). D-NMR (400 MHz): 2.815 – 2.426 (*m*, *J* = 123.9, CHDCOO); 1.264 (*d*, *J* = 126.7, CH$_2$D). MALDI-MS: 2141 ([*M* + Na + K]$^+$), 2117 ([*M* + K]$^+$), 2101 ([*M* + Na]$^+$), 2009 ([*M* – Bn]$^+$), 1925 ([*M* – 1 HB]$^+$), 1839 ([*M* – 2 HB]$^+$), 1753 ([*M* – 3 HB]$^+$), 1667 ([*M* – 4 HB]$^+$), 1581 ([*M* – 5 HB]$^+$), 1495 ([*M* – 6 HB]$^+$), 1409 ([*M* – 7 HB]$^+$), 1323 ([*M* – 8 HB]$^+$), 1587, 1501, 1415, 1329, 1243, 1232, 1155, 1063, 977, 891, 807, 801, 721, 715, 635, 629, 543, 453.

REFERENCES

[1] Y. Doi, 'Microbial Polyesters', VCH, Weinheim, 1990; A. Steinbüchel, in 'Biomaterials', Ed. D. Byrom, Stockton Press, New York, 1991, p. 123 – 213; H. G. Schlegel, 'Allgemeine Mikrobiologie', 7th edn., Thieme Verlag, Stuttgart, 1992.

[2] D. Seebach, A. Brunner, H. M. Bürger, R. N. Reusch, L. L. Bramble, *Helv. Chim. Acta* **1996**, *79*, 507; S. Das, U. D. Lengweiler, D. Seebach, R. N. Reusch, *Proc. Natl. Acad. Sci. U.S.A.* **1997**, *94*, 9075; S. Das, R. N. Reusch, *Biochemistry* **2001**, *40*, 2075.

[3] M. G. Fritz, P. Walde, D. Seebach, *Macromolecules* **1999**, *32*, 574.

[4] R. N. Reusch, H. Sadoff, *Proc. Natl. Acad. Sci. U.S.A.* **1988**, *85*, 4176; R. N. Reusch, *Proc. Soc. Exp. Biol. Med.* **1989**, *191*, 377.

[5] M. Yokouchi, Y. Chatani, H. Tadokoro, H. Tani, K. Teranishi, *Polymer* **1973**, *14*, 267; J. S. Pazur, S. Raymond. P. J. Hocking, R. H. Marchessault, *Polymer* **1998**, *39*, 3065; J. S. Pazur, S. Raymond, P. J. Hocking, R. H. Marchessault, *Macromolecules* **1998**, *31*, 6585.
[6] D. Seebach, H. M. Bürger, H.-M. Müller, U. D. Lengweiler, A. K. Beck, K. E. Sykes, P. A. Parker, P. J. Barham, *Helv. Chim. Acta* **1994**, *77*, 1099; K. E. Sykes, T. J. McMaster, M. J. Miles, P. A. Parker, P. J. Barham, D. Seebach, H.-M. Müller, U. D. Lengweiler, *J. Mat. Sci.* **1995**, *30*, 623.
[7] D. A. Plattner, A. Brunner, M. Dobler, H.-M. Müller, W. Petter, P. Zbinden, D. Seebach, *Helv. Chim. Acta* **1993**, *76*, 2581; D. Seebach, T. Hoffmann, F. N. Kühnle, U. D. Lengweiler, *Helv. Chim. Acta* **1994**, *77*, 2007.
[8] M. Rueping, A. Dietrich, V. Buschmann, M. G. Fritz, M. Sauer, D. Seebach, *Macromolecules* **2001**, in press.
[9] H.-M. Müller, D. Seebach, *Angew. Chem.* **1993**, *105*, 483; *Angew. Chem., Int. Ed.* **1993**, *32*, 477; D. Seebach, A. Brunner, B. M. Bachmann, T. Hoffmann, F. N. Kühnle, U. D. Lengweiler, 'Ernst Schering Research Foundation', Vol. 28, 1995; D. Seebach, M. G. Fritz, *Int. J. Biol. Macromol.* **1999**, *25*, 217.
[10] D. Seebach, U. Brändli, P. Schnurrenberger, M. Przybylski, *Helv. Chim. Acta* **1988**, *71*, 155.
[11] H. M. Müller, Diss. ETH, Nr. 9685, Zürich, 1992; U. D. Lengweiler, M. G. Fritz, D. Seebach, *Helv. Chim. Acta*, **1996**, *79*, 670; B. M. Bachmann, D. Seebach, *Helv. Chim. Acta* **1998**, *81*, 2430.
[12] R. Noyori, M. Kitamura, '*Enantioselective Catalysis with Metal Complexes. An Overview*'; in 'Modern Synthetic Methods', Vol. 5, Heidelberg, Springer-Verlag, 1989, p. 115–198.
[13] J. P. Genêt, C. Pinel, V. Ratovelomanana-Vidal, S. Mallart, X. Pfister, L. Bischoff, M. C. C. D. Andrade, S. Darses, J. A. Laffite, *Tetrahedron: Asymmetry* **1994**, *5*, 675.
[14] D. Seebach, U. Gysel, K. Job, A. K. Beck, *Synthesis* **1992**, 39.
[15] D. Seebach, J. Zimmermann, U. Gysel, R. Ziegler, T. K. Ha, *J. Am. Chem. Soc.* **1988**, *110*, 4763.
[16] Y. Noda, D. Seebach, *Helv. Chim. Acta* **1987**, *70*, 2137; J. Zimmermann, D. Seebach, *Helv. Chim. Acta* **1987**, *70*, 1104.
[17] J. Li, J. Uzawa, Y. Doi, *Bull. Chem. Soc. Jpn.* **1997**, *70*, 1887; J. Li, J. Uzawa, Y. Doi, *Bull. Chem. Soc. Jpn.* **1998**, *71*, 1683.
[18] B. Reif, M. Hennig, C. Griesinger, *Science* **1997**, *276*, 1230; D. Yang, R. Konrat, L. E. Kay, *J. Am. Chem. Soc.* **1997**, *119*, 11983; H. Schwalbe, T. Carlomagno, M. Hennig, J. Junker, B. Reif, C. Richter, C. Griesinger, 'Cross-Correlated Relaxation for the Measurement of Angles between Tensorial Interactions', *Methods Enzymol* **2001**, in press.
[19] B. A. Cornell, *J. Chem. Phys.* **1996**, *85*, 4199.
[20] C. Griesinger, U. Eggenberger, *J. Magn. Reson.* **1992**, *97*, 426.

Received April 20, 2001